

Study of effects of the crystal field in intermetallic rare-earth compounds by inelastic neutron scattering

A. Andreeff, L. P. Kaun, and T. Frauenheim

Joint Institute for Nuclear Research, Dubna

B. Lippold

Karl Marx University, Leipzig

W. Matz

Central Institute of Nuclear Research, GDR Academy of Sciences, Rossendorf
 Fiz. Elem. Chastits At. Yadra **12**, 277-323 (March-April 1981)

The results of inelastic magnetic scattering of neutrons in intermetallic compounds of rare earths are reviewed. The paper consists of two parts. In the first, single-particle excitations are considered, and the various compounds are classified according to the lattice structure. The obtained results are analyzed by means of a phenomenological theory of the crystal field with a view to determining its parameters. These parameters are compared within isostructural compounds. The second part of the paper is devoted to collective excitations which lead to magnetic phase transitions and the Jahn-Teller effect.

PACS numbers: 75.30.Kz, 71.70.Ch, 75.25.+z, 76.80.+y

INTRODUCTION

The rare earths and their compounds are currently among the most intensively investigated groups of elements of the periodic table. They have the electron structure

$$[\text{Xe}, (4f)^n].$$

The radial charge distribution given in Fig. 1 shows that the 4f electrons are deep within the xenon core. They are screened by 5s and 5p electrons and are strongly localized. The crystal environment acts on the 4f electrons in a manner equivalent to an external electric field. This electric field is produced by the charge distribution near the considered ion, the distribution depending, on the one hand, on the charge state of the ligand and, on the other, on the crystal symmetry. Under the influence of this external field, the M_J degeneracy of the energy states of the 4f electrons of the free ion is lifted (this is a special case of the Stark effect), which leads to the occurrence of the so-called crystal-field levels.

The typical splitting of the electron multiplets in metallic rare-earth compounds is of order 20 meV. This corresponds to a temperature $\sim 220^\circ\text{K}$. The crystal-field levels are separated from one another by about 5.5 meV, which in temperature units corresponds to 60°K . Compared with the interactions of the electrons with one another and with the nucleus in the free ion (>1 eV), the crystal field can be regarded as a perturbation. The resulting fine structure of the electron multiplets affects the physical properties and processes in the solid (crystal-field effects), which exhibit a definite dependence on the energy spacings, the nature of the levels, and their populations.

The investigation of crystal-field effects began to develop strongly at the end of the forties. Such studies were particularly stimulated by the development of solid-state masers and lasers, the principle of their action being intimately related to the properties of the

crystal-field levels.¹ They also have a direct bearing on the technique of obtaining superlow temperatures ($T < 1^\circ\text{K}$) by means of adiabatic demagnetization.² A large fraction of the experimental results were obtained by optical investigations (absorption and fluorescence spectra³ and infrared spectroscopy⁴). Because of their high energy resolution, these methods make it possible to determine level energies with accuracy as good as 0.1 meV. Through polarization measurements⁵ and study of the fine structure of the optical lines one can obtain additional information about the properties of the crystal-field levels and the coupling of the crystal field to the lattice vibrations.

Independent conclusions about the positions of the crystal-field levels and their characteristics can be obtained by measuring the temperature dependence of various macroscopic properties.⁶ The fine structure of the ground-state multiplet is manifested in the specific heat through the Schottky anomaly. In the general definition, the specific heat is expressed by

$$C = \partial U / \partial T, \quad (1)$$

where U is the internal energy of the system and T is the temperature. If one considers only the system of

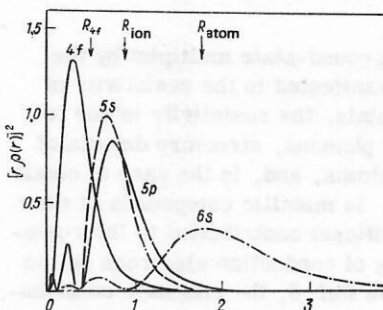


FIG. 1. Radial distribution of the charge density for the 4f, 5s, 5p, and 6s electrons of the Gd^{3+} ion.⁷

the 4f electrons, then its internal energy is

$$U = \frac{1}{Z} \sum_n g_n E_n \exp(-E_n/kT). \quad (2)$$

Here, $Z = \sum_n g_n \exp(-E_n/kT)$ is the partition function of the system, and g_n is the degeneracy of level n . From this we obtain the expression for the Schottky anomaly:

$$C_{\text{Schottky}} = \frac{1}{Z^2 k T^2} \left[Z \sum_n g_n E_n^2 \exp(-E_n/kT) - \left(\sum_n g_n E_n \exp(-E_n/kT) \right)^2 \right]. \quad (3)$$

The entropy of the ion at high temperature is

$$S = k \ln \left(\sum_n g_n \right). \quad (4)$$

The gain in the entropy by an increase in the temperature is

$$\Delta S = S - k \ln g_1 = \int_0^\infty \frac{1}{T} C_{\text{Schottky}} dT. \quad (5)$$

This gain in the entropy can be determined by numerical integration of the curve of the experimentally measured specific heat, which gives a criterion for determining the degree of degeneracy of the ground state.

The magnetic susceptibility gives some information about the fine structure of the ground-state multiplet. It follows from statistical thermodynamics that

$$\chi = \partial^2 F / \partial H^2|_{H=0}, \quad (6)$$

where F , the free energy, is determined by

$$F = -kT \ln Z$$

(Z depends on the magnetic field H). The energy E_n of the n -th electron state is obtained by perturbation theory:

$$E_n = E_n^0 + \mu_B g H \langle n | J | m \rangle + \mu_B^2 g^2 H^2 \sum_{n \neq m} \frac{| \langle n | J | m \rangle |^2}{E_n^0 - E_m^0}. \quad (7)$$

Thus, the magnetic susceptibility is given by the expression

$$\chi(T) = \frac{N \mu_B^2 g^2}{Z} \left\{ \sum_n \frac{| \langle n | J | m \rangle |^2}{kT} \exp(-E_n/kT) + 2 \sum_{n \neq m} \frac{| \langle n | J | m \rangle |^2}{E_n^0 - E_m^0} \exp(-E_n/kT) \right\}. \quad (8)$$

The Curie term of the susceptibility depends on the diagonal matrix elements. If the ground-state diagonal elements are zero ($\langle n | J | n \rangle = 0$), magnetic ordering is not manifested even at very low temperatures. In this case, the susceptibility does not depend on the temperature. Compounds with this property are called Van Fleck paramagnets.

The splitting of the ground-state multiplet by the crystal field is also manifested in the resistivity of metals. In normal metals, the resistivity is due to electron scattering by phonons, structure defects of the lattice, impurity atoms, and, in the case of small samples, the surface. In metallic compounds of rare earths there is an additional contribution to the resistivity due to scattering of conduction electrons on the crystal-field levels. In Ref. 8, the magnetic contribution to the resistivity per ion is calculated:

$$\rho_m = \rho_0 \text{Sp}(P \cdot Q). \quad (9)$$

The matrices P and Q contain the energies E_n of the crystal-field levels and their wave functions $|n\rangle$:

$$P_{nm} = \frac{\exp(-E_n/kT)}{Z} \frac{(E_m - E_n)/kT}{1 - \exp[(E_n - E_m)/kT]}; \quad (10)$$

$$Q_{nm} = | \langle n | J_z | m \rangle |^2 + (1/2) (| \langle n | J_+ | m \rangle |^2 + | \langle n | J_- | m \rangle |^2). \quad (11)$$

The resistivity depends in a complicated manner on the crystal-field levels. It is very difficult to draw unambiguous conclusions about the scheme of these levels from such measurements.

In the last ten years, inelastic scattering of neutrons has been successfully used as a method for investigating crystal-field effects. This method gives direct data about the positions of the crystal-field energy levels. The differential cross section for scattering of neutrons from the state $|k\rangle$ to the state $|k'\rangle$ by a nucleus with change in the state of this nucleus in the sample from $|\lambda\rangle$ to $|\lambda'\rangle$ is given by the general expression¹⁴

$$\left(\frac{d^2\sigma}{d\Omega dE} \right)_{k'\lambda'} = \frac{k'}{k} \left(\frac{m}{2\pi\hbar^2} \right)^2 | \langle k' \lambda' | \hat{V} | k \lambda \rangle |^2 \delta(E + E_k - E_{\lambda'}). \quad (12)$$

To obtain the differential cross section for all possible scattering processes, it is necessary to sum over all final states $|\lambda'\rangle$ and over all initial states $|\lambda\rangle$, which have probability P_λ :

$$\frac{d^2\sigma}{d\Omega dE} = \frac{k'}{k} \left(\frac{m}{2\pi\hbar^2} \right)^2 \sum_{\lambda, \sigma} P_\lambda P_\sigma \times \sum_{\lambda', \sigma'} | \langle k' \sigma' \lambda' | \hat{V} | k \sigma \lambda \rangle |^2 \delta(E + E_k - E_{\lambda'}). \quad (13)$$

The summation over σ and σ' takes into account the fact that the neutron beam is not polarized. The relation (13) is fundamental for the description of any scattering process. The individual scattering processes are characterized by a definite form of the interaction potential \hat{V} . However, in any case it can be assumed that \hat{V} is a function of the distance of the neutron from the target nucleus:

$$V(r) = \sum_j \hat{V}_j(r - R_j). \quad (14)$$

Here, the sum over j denotes summation over all nuclei. In such a case, the scattering cross section can be written in the form of two factors:

$$\frac{d^2\sigma}{d\Omega dE} = \frac{k'}{k} \left(\frac{m}{2\pi\hbar^2} \right)^2 | \hat{V}(\kappa) |^2 S(\kappa, \omega). \quad (15)$$

The quantity $V(\kappa) = \int dr \exp(-i\kappa \cdot r) V(r)$ depends only on the two-particle potential and is determined by the definite form of the interaction. The correlation function $S(\kappa, \omega)$ contains a form factor and describes the correlation of the system for a definite nature of the interaction (magnetic or nuclear scattering).

Besides nuclear scattering, one of the main processes of interaction of neutrons with rare-earth compounds is magnetic scattering by the 4f electrons. In this process, energy is transferred from a neutron to an electron or vice versa, and the electron system goes over to a different energy state. The positions of the peaks in the inelastic neutron scattering spectrum correspond to definite transition energies, and their intensities are proportional to the transition probabilities. For nonconducting compounds, the inelastic neutron scattering method is a good complement to the optical investigations. In contrast to the latter, inelastic neutron scat-

tering is not used to investigate electric dipole transitions between the crystal-field levels of the ground-state multiplet to higher-lying multiplets but rather to study magnetic dipole transitions between the crystal-field levels of the ground-state multiplet. The inelastic neutron scattering does not depend on the optical absorption properties of the material of the sample. This last circumstance is particularly important in the study of crystal-field effects in metallic compounds. Because of the strong absorption by conduction electrons, the optical methods of investigation in the case of metals are virtually useless, and inelastic neutron scattering is as yet the only means for observing the crystal-field levels. The task of the investigations of metallic compounds of the rare earths is to obtain a sufficient number of experimental data on the splitting of the energy levels under the influence of the crystal field. The experimental results are analyzed by means of a phenomenological theory of the crystal field with a view to determining its parameters (see Sec. 1). The values of the parameters and comparison of them within, for example, a series of isostructural compounds give definite information about the properties of the metallic matrix in which the rare-earth ions are contained. The coupling of the magnetic rare-earth ions to one another leads to a number of features that cannot be encompassed by a relatively simple description (see Sec. 3). It is helpful to divide the intermetallic compounds of the rare-earth elements into two large groups. In the first, the partner rare-earth element is nonmagnetic, while in the second group the partner has a magnetic moment. The magnetic properties of the first group are completely determined by the interaction between the rare-earth ions. In the second group, one must in principle distinguish three types of interaction: the rare-earth-rare-earth interaction, the rare-earth-magnetic-partner interaction, and the interaction between the magnetic ions of the rare-earth partners. To study the second group, it is necessary to know accurately the coupling of the first and third types of interaction. Therefore, inelastic neutron scattering has hitherto been used mainly to investigate intermetallic compounds of the first group.

1. FUNDAMENTALS OF THE DESCRIPTION OF THE CRYSTAL FIELD^{6,12}

There is at present no satisfactory microscopic theory of the crystal field, and one therefore uses a phenomenological description of it by means of equivalent operators. The equivalent operators are formal transformations made to facilitate calculations. The potential of the crystal field is represented as a series in spherical functions, which depend on the spatial coordinates x, y, z . The task of the calculations is to determine the eigenvalues of the $4f$ electrons in the crystal field, for which it is necessary to determine the matrix element by means of the $4f$ wave function. The angular part of a wave function is characterized by the total angular momentum and its projection. In the spherical functions, which are tensor operators, one can replace the coordinates by the corresponding components of the operator of the total angular momentum. One then obtains the equivalent operators O_l^m , which

are functions of only the operator of the angular momentum and its components. It is assumed that a restriction can be made to a single isolated multiplet (for example, the ground-state multiplet) of the rare-earth ion, and its splitting in the electric field is investigated. The total angular momentum $J(J=L+S)$ is regarded as a good quantum number, and the operator of the crystal-field Hamiltonian is written in the form⁹

$$H_{cf} = \sum_{l=2,4,6} \sum_{m=0}^l B_l^m O_l^m(J, J_z, J_z). \quad (16)$$

The crystal-field parameters B_l^m contain information about the crystal field as follows. The number of nonvanishing B_l^m determines the symmetry of the field. The higher the symmetry, the smaller the number of nonvanishing parameters of the crystal field. The values of B_l^m determine the strength of the field. The relative values of the B_l^m determine the form of the multiplet splitting, i.e., the order in which the crystal-field levels follow one another.

The summation over l is restricted to $l=2, 4, 6$ because only the $4f$ electrons of the rare-earth ions are considered. To illustrate the dependence of the number of terms in the operator of the crystal-field Hamiltonian on the symmetry, we give the Hamiltonian operators for cubic symmetry and hexagonal point symmetry:

$$\begin{aligned} H_{cf, \text{cub}} &= B_4^0 [O_4^0 + 5O_4^4] + B_6^0 [O_6^0 - 21O_6^4]; \\ H_{cf, \text{hex}} &= B_4^0 O_4^0 + B_4^4 O_4^4 + B_6^0 O_6^0 + B_6^4 O_6^4. \end{aligned} \quad (17)$$

In Refs. 10 and 11, these Hamiltonian operators were used to calculate and tabulate the splitting of the multiplets in a cubic and a hexagonal crystal field with all the J values observed in rare-earth ions ($2 \leq J \leq 8$).

The parameters B_l^m can be divided into definite constituent parts which reveal more clearly the contributions from the crystal field itself and the rare-earth ion, which serves as a probe for measuring the crystal field:

$$B_l^m = A_l^m \langle r^l \rangle K_l^m \Theta_l. \quad (18)$$

Here, Θ_l are reduced matrix elements, tabulated for all the rare-earth ions¹²; $\langle r^l \rangle$ are radial integrals of the wave functions of the $4f$ electrons, which take different values depending on the method of calculation (nonrelativistic⁷ or relativistic¹³). The parameters A_l^m contain the actual information about the crystal field produced by the charge environment of the probe. Since the K_l^m are only numerical factors, we shall include them in the A_l^m and write $A_l^m = A_l^m K_l^m$. To compare the crystal parameters of different compounds, one should take the $A_l^m \langle r^l \rangle$ or only the A_l^m .

2. DETERMINATION OF THE CRYSTAL-FIELD PARAMETERS IN RARE-EARTH INTERMETALLIC COMPOUNDS BY INELASTIC NEUTRON SCATTERING

The model of effective point charges or modifications of it are used to determine the parameters of the electric crystal field. In this model, the electric field at the position of an atom in the crystal is determined by the total potential of all the neighboring ions, which are regarded as point charges situated at the positions of

the nuclei.

Below, we give a review of the crystal-field parameters for metallic and intermetallic rare-earth compounds determined primarily by inelastic neutron scattering. For completeness, we also give in some cases the results of other methods of investigation of the crystal field. It should be noted that hitherto the investigations have concentrated on compounds with cubic crystal structure. For hexagonal compounds, there are some first results of the systematic determination of the crystal-field parameters, but for compounds with lower symmetry there are virtually no neutron-scattering results.

Before we begin the exposition of the results, we modify the general expression (15) for the scattering cross section. To analyze experiments in which the crystal field is investigated by inelastic neutron scattering, the scattering cross section in the dipole approximation has the form¹⁵

$$\frac{d^2\sigma}{d\Omega dE} = \left(\frac{1.94e^2}{2m_0c^2} g_J \right)^2 \frac{k'}{k} f^2(\kappa) \times \sum_{n, m} P_n |\langle n | J_{\perp} | m \rangle|^2 \sqrt{\frac{4 \ln 2}{\pi \gamma_{nm}^2}} \left[-4 \ln 2 \left(\frac{E_n - E_m - E}{\gamma_{nm}} \right)^2 \right]. \quad (19)$$

Here, $|n\rangle$ are the wave functions of the crystal levels with energies E_n ; $f(\kappa)$ is the magnetic form factor of the rare-earth ion; and $\kappa = k - k'$ is the momentum-transfer vector. In the experiments, one observes transitions between crystal-field levels with energy transfer E from the neutrons and transition half-widths γ_{nm} .

The intensity of the individual peaks is proportional to the matrix element, which in the case of polycrystalline samples is given by the expression (dipole approximation)

$$|\langle n | J_{\perp} | m \rangle|^2 = (1/3) \{ |\langle n | J_+ | m \rangle|^2 + |\langle n | J_- | m \rangle|^2 + 2 |\langle n | J_z | m \rangle|^2 \}. \quad (20)$$

The probability P_n that the system is in the state $|n\rangle$ is given by the population factor of the crystal-field levels, which satisfies Boltzmann statistics:

$$P_n = \exp(-E_n/kT) / \sum_{n=1}^{2J+1} \exp(-E_n/kT). \quad (21)$$

The expression (21) for the scattering cross sections is valid only for small momentum transfers ($\kappa \rightarrow 0$). Therefore, in an analysis of the experiments it is important to know the upper limit on the κ values for which (21) can be used without introducing gross errors. For Pr^{3+} in a cubic crystal field, the expression for the total cross section for neutron scattering with transitions between the crystal levels was considered in Ref. 16. The results of Ref. 16 are compared with the calculation based on Eq. (20) in Fig. 2. It can be seen that when $\kappa > 5.5 \text{ \AA}^{-1}$ the deviations from the exact value are greater than 1%.

Comparing the spacings between the positions of the crystal-field levels and the transition probabilities calculated by means of the theory with the positions of the peaks and their intensities in the experimental spectrum of inelastically scattered neutrons, one can determine the set of crystal-field parameters for the in-

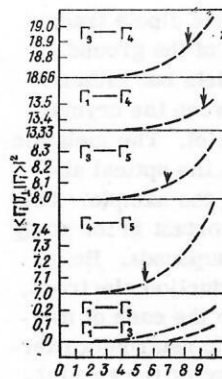


FIG. 2. Probabilities of transitions between the crystal levels in a cubic field as functions of the momentum transfer κ for Pr^{3+} .

vestigated material. Provided the half-widths γ_{nm} remain small (1–2 meV) and well resolved peaks are observed in the spectrum, inelastic neutron scattering is a very sensitive method for determining the crystal-field parameters.

2.1. Investigation of the crystal field in rare-earth compounds with cubic crystal structure

In this subsection we discuss the investigation of the crystal field in metallic and intermetallic rare-earth compounds with cubic structure. We restrict ourselves to four types of cubic structure, for which there are various results that reveal definite tendencies.

Structure of NaCl(BI) type. The compounds with V and VI elements of the principal subgroups of the periodic rare-earth elements (pnictides and chalcogenides) with 1:1 ratio of the atoms have NaCl-type structure. From the point of view of the study of the crystal field, they are the group of materials which have been most systematically investigated. The neutron scattering experiments on PrBi (Fig. 3, Ref. 18) were the first that made it possible to determine the crystal-field parameters, and they marked the beginning of inelastic neutron scattering in the systematic investigation of the crystal field in metallic rare-earth systems. The monochalcogenides and monpnictides of the rare-earth metals have metallic properties up to the nitrides. For

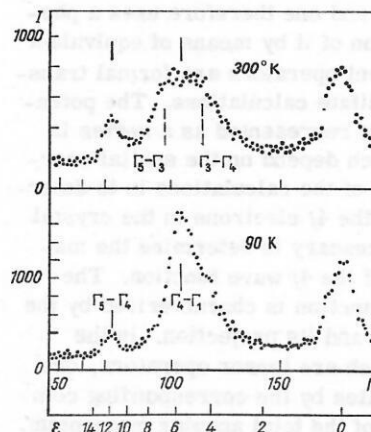


FIG. 3. Time-of-flight neutron spectrum for PrBi .¹⁸

	N	P	As	Sb	Bi	S	Se	Te
Ce								
Pr								
Nd								
Pm								
Sm								
Eu								
Gd								
Tb								
Dy								
Ho								
Er								
Tm								
Yb								

FIG. 4. Monopnictides and monochalcogenides of rare-earth elements for which inelastic neutron scattering has been used to determine the crystal-field parameters.

the pnictides, because of their position in the periodic table, one would expect them to form $A^{III}B^V$ -type semiconductors. The resistivity at room temperature is of order 10^{-3} – $10^{-4} \Omega \cdot \text{cm}$, i.e., it is in the typical metallic range of carrier densities, though 1–2 orders of magnitude lower than in the chalcogenides.¹⁹

Rare-earth compounds with NaCl structure are well suited to study of the crystal field, since the interaction of the magnetic ions with the crystal field in them is much greater than the magnetic exchange interaction. This is expressed in the absence of magnetic order or in a very low ordering temperature ($<20^\circ\text{K}$). Figure 4 shows the compounds for which the crystal-field parameters have been determined by inelastic neutron scattering. (The values for the samarium compounds are taken from measurements of the Schottky anomaly.) Most of the experiments were made by Birgeneau *et al.* using a time-of-flight spectrometer with a chopper,^{18–21} and also by Furrer *et al.* with a triple-axis spectrometer^{22–25} and MARX spectrometer.²⁶

On the basis of the above, two questions can be posed.

1. How do the crystal-field parameters change if the partner of the rare-earth ion in the compound is changed?
2. How do the crystal-field parameters change if the rare-earth ion in a compound is changed, the partner remaining the same?

With regard to the first question, a systematic investigation into praseodymium compounds was made in Ref. 19. For neodymium compounds, there are also experimental data for the crystal-field parameters, so that here too such an analysis can be made. All the compounds are characterized by a predominant contribution of the term of fourth order to the crystal potential. Comparison of the crystal-field parameters of fourth order with one another for both the praseodymium compounds and the neodymium compounds does not reveal significant differences between the monochalcogenides and monopnictides, although the two groups have different carrier densities. The nitrides are an exception which are more semiconductors than metals. The dependence of the values of $A_4\langle r^4 \rangle$ on a^{-5} (a is the

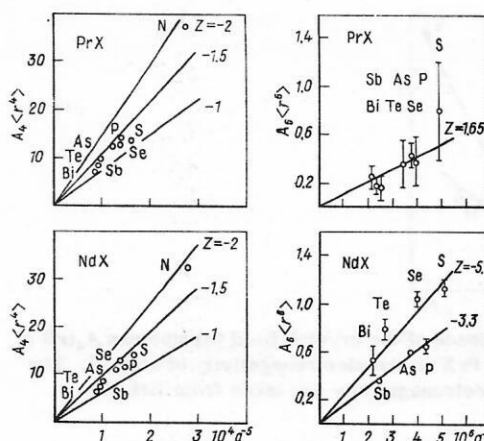


FIG. 5. Crystal-field parameters of the monochalcogenides and monopnictides of praseodymium and neodymium as functions of the power of the lattice constant a . The points are the experimental data, and the lines correspond to the point-charge model.

lattice constant) indicates that the lattice constant is the basic characteristic parameter (Fig. 5). Such a dependence is expected in the model of point charges, in which the crystal-field parameters for NaCl structure with allowance for the neighbors of the first coordination sphere are described by¹²

$$A_4\langle r^4 \rangle = -\frac{7}{16} \frac{Ze^2}{R^5} \langle r^4 \rangle; \quad A_6\langle r^6 \rangle = -\frac{3}{64} \frac{Ze^2}{R^7} \langle r^6 \rangle, \quad (22)$$

where Z is the charge of the ligand, and R is the distance to the neighboring atom ($R = a/2$ for NaCl structure). It is noteworthy that the crystal-field parameters of fourth order can even be calculated with good quantitative accuracy in the model of point charges if one takes $Z = 1.2 \pm 0.1$ for the charge of the ligand and the relativistic radial integrals¹³ (see Fig. 5). To some extent, this is unexpected, since this model gives poor quantitative predictions for insulators.²⁷ In metallic compounds, besides the mechanisms that influence the crystal field in insulators (the effect of the point charge, charge penetration, covalence, and 5s and 5p screening), there must be screening effects of the virtually bound 5d state because of the presence of the conduction electrons. Nevertheless, the point-charge model "works" without allowance for the additional effects.

It can be seen from Fig. 5 that for the praseodymium compounds $A_6\langle r^6 \rangle$ is also a linear function of a^{-7} to within the experimental errors. However, the neodymium compounds exhibit a difference between the pnictides and chalcogenides greater than the experimental errors. In the neodymium monochalcogenides, the contribution to the crystal field of sixth order is greater than in the monopnictides. The effective charge for the praseodymium compounds is $Z = -1.65$, for the neodymium monopnictides $Z = -3.3$, and for the neodymium monochalcogenides $Z = -5.1$ if the relativistic radial integrals $\langle r^6 \rangle$ are used. The different values of the charges for the parameters of fourth and sixth order indicate that the screening effects and the contribution from the covalent bonding are more clearly manifested in the sixth order of the crystal-field potential. In this

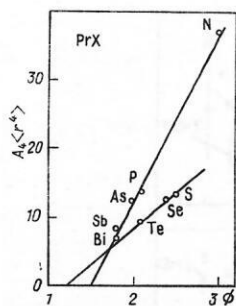


FIG. 6. Dependence of the crystal-field parameters $A_4\langle r^4 \rangle$ of the compounds PrX on the electronegativity of atom X. The values of the electronegativity are taken from Ref. 29.

sense, one can also understand the different behavior of $A_6\langle r^6 \rangle$ for the neodymium monpnictides and monochalcogenides, i.e., the valence electrons have a definite influence in them.¹⁹ The equality of the crystal-field parameters of sixth order for the praseodymium chalcogenides and pnictides is to be regarded as an exception.

On the basis of the good agreement between the values of $A_4\langle r^4 \rangle$ and calculations based on the point-charge model and also the absence of an indication of an influence of the conduction electrons, Bucher and Maita²⁸ attempted to explain the crystal-field parameters in an atomistic approach. Representation of the sixth-order crystal-field parameters as functions of the electronegativity of the partner (Fig. 6) reveals a linear dependence and, in addition, a separation into pnictides and chalcogenides. The electronegativity of the X atom is too small to attract all the three praseodymium electrons, so that these compounds are metals, whereas nitrogen, with greater electronegativity, forms non-metallic compounds.

We now consider the second question—the change in the crystal-field parameters when the rare-earth ion in the compounds is changed. Figure 7 shows the modified parameters $A_n\langle r^n \rangle a^{n+1}$ for rare-earth pnictides.²¹ One notes clearly the anomalous behavior of the cerium compounds, whose $A_4\langle r^4 \rangle$ values are clearly lower than for the neighboring rare earths. This is explained by the fact that the individual 4f electron of the

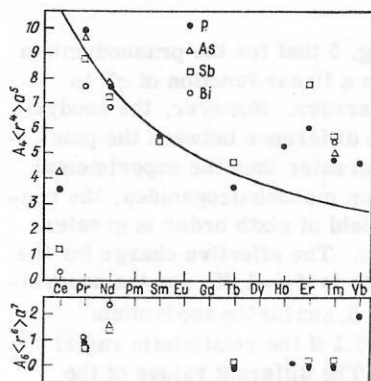


FIG. 7. Crystal-field parameters of compounds of rare-earth elements with the atom X (X = P, As, Sb, Bi). The points are the experimental data, and the curve corresponds to the point-charge model.

Ce atom is near the Fermi limit with a large probability. For the fourth-order parameters of the other compounds one observes a certain systematic trend through the rare-earth series. The continuous curve is obtained from calculations in accordance with the model of effective point charges by means of the expression (22), $Z = -1.2$, and the relativistic values for $\langle r^4 \rangle$. The agreement with the experimental parameters from Pr to Tb is very good. For the heavier rare-earth ions, $Z = -2$ would reproduce the measured values better. An abrupt change in the electron properties of the compounds in the series is, however, improbable, and the observed behavior is more likely to be an indication of the imperfection of the point-charge model. It is as yet difficult to indicate the mechanism responsible for this. The increasing fraction of the covalent bond is the most probable.²¹

For the sixth-order parameters, with relatively large errors, a constant value was found for $A_6\langle r^6 \rangle a^7 \approx (0.1 \pm 0.06) \times 10^6 \text{ meV} \cdot \text{\AA}^7$ [by means of (3.4)] (see Fig. 7). This means that the model of effective point charges is not suitable for calculating $A_6\langle r^6 \rangle$. It is only useful for a qualitative estimate of the order of magnitude of the crystal-field parameters.

Structure of CsCl (B2) type. Compounds of the rare-earth elements with rhodium, palladium, copper, silver, zinc, and magnesium crystallize in a CsCl(B2) structure. They are the group of materials that have been studied next best. A structure of CsCl type is well suited for a study of the dependence of the crystal-field parameters on the valence and size of the atoms of the ligands, and also the electron structure in an isomorphic series of intermetallic compounds. The majority of the results on this group of materials was obtained by Morin, Pierre, *et al.*³¹⁻³⁵ The experimental methods included, besides inelastic neutron scattering, measurement of the magnetic anisotropy in single crystals,³³ neutron diffraction determination of the magnetic structure, and study of the magnetoelastic properties.³⁶

In the intermetallic compounds, the magnetic exchange interaction is more strongly manifested along-

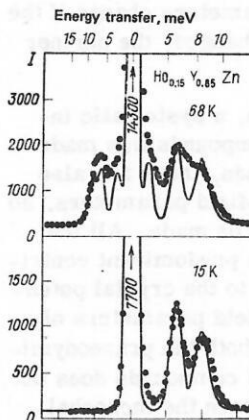


FIG. 8. Neutron-scattering spectrum for the compound $\text{Ho}_{0.15}\text{Y}_{0.85}\text{Zn}$ measured with the time-of-flight spectrometer IN-7 (ILL Grenoble). The curves are the theoretical fitting of Ref. 33.

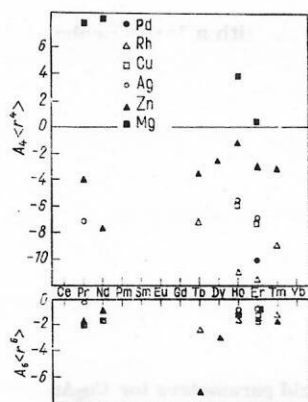


FIG. 9. Crystal-field parameters for intermetallic compounds with CsCl structure.

side the interaction with the crystal field. This is reflected in an ordering temperature of 40°K or higher for many compounds. To reduce the exchange interaction in the neutron scattering experiments, it is customary to use dilute compounds.³¹⁻³³ Figure 8 shows a typical spectrum of the scattered neutrons for CsCl compounds.

Figure 9 shows the crystal-field parameters found for this series of compounds. The investigation concentrated not so much on the change of the crystal-field parameters due to the rare-earth ion as on the influence of the partner in the compound on the strength of the crystal field for one definite ion of the rare-earth metals. The most complete results are available for the compounds of erbium^{31,32} and holmium.³³ In Table I, we give the parameters for both series of compounds.

It can be seen that the fourth-order parameters are predominantly negative and decrease in absolute magnitude with the change in the number of external electrons of the partner in the sequences Rh, Pd, Ag and Cu, Zn, and Mg. For magnesium, the value of $A_4\langle r^4 \rangle$ becomes positive. The values of the parameters for isoelectron compounds are not apparently affected by the change in the lattice constant. The sixth-order parameters are all negative and have the same order of magnitude. Compared with the NaCl-type compounds, the contribution of the sixth-order potential in the case of CsCl-type compounds is appreciably greater.

Attempts to calculate the crystal-field parameters by means of the point-charge model³¹ with allowance for the second coordination sphere (ions of the rare-earth elements) led to a negative value of the charge of the ligands in the cases of Cu and Ag and $Z \approx 0$ for Zn with good reproduction of the $A_4\langle r^4 \rangle$ values. However, the $A_6\langle r^6 \rangle$ values were then underestimated by an entire

TABLE I. Crystal-field parameters (meV) of intermetallic compounds of holmium and erbium with CsCl-type structure.³⁰⁻³³

Partner	Holmium		Erbium	
	$A_4\langle r^4 \rangle$	$A_6\langle r^6 \rangle$	$A_4\langle r^4 \rangle$	$A_6\langle r^6 \rangle$
Rh	-10.77 ± 1.6	-1.55 ± 0.26	-10.6 ± 0.9	-1.62 ± 0.09
Pd	—	—	-10.08	-1.02
Ag	-5.77 ± 0.060	-1.03 ± 0.09	-6.3 ± 0.3	-1.8 ± 0.04
Cu	-5.86 ± 0.69	-1.29 ± 0.09	-7.25 ± 0.55	-1.3 ± 0.09
Zn	-1.21 ± 0.34	-1.55 ± 0.09	-3.14 ± 0.040	-1.54 ± 0.09
Mg	3.62 ± 0.78	-1.12 ± 0.09	0.31 ± 0.25	-0.93 ± 0.09

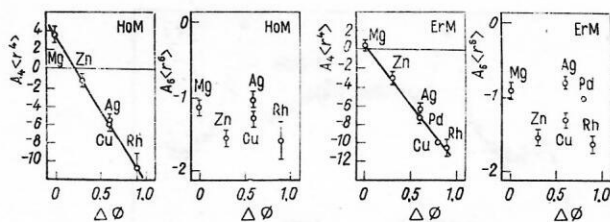


FIG. 10. Crystal-field parameters of compounds of holmium and erbium with CsCl-type structure as functions of the electronegativity difference. The values of the electronegativity are taken from Ref. 19.

order of magnitude. As a result, the point-charge model for compounds with CsCl structure loses its practical value for qualitative determination of the crystal-field parameters. It is noteworthy that for the fourth-order parameters one obtains a linear dependence on the difference between the electronegativity of the ions of the rare-earth metals and the ligands (Fig. 10). This last circumstance is regarded as an indication of charge transfer in these compounds.³² In contrast, the parameters $A_6\langle r^6 \rangle$ do not satisfy any such dependence (see Fig. 10).

To explain the changes in the crystal-field parameters in the holmium and erbium compounds, some theoretical investigations were made into the part played by the conduction electrons in forming the crystal field.³⁷ According to calculations using orthogonalized plane waves as wave functions, the contribution of the effective charge of the ligands is very small ($|A_4\langle r^4 \rangle| < 1$ meV; $A_6\langle r^6 \rangle \approx -0.1$ meV). The calculations showed that because of the anisotropic distribution of the conduction electrons one obtains a direct Coulomb contribution, which gives in absolute magnitude the correct order of $A_4\langle r^4 \rangle$, and also its dependence on the type of partner. The reason for the change in $A_4\langle r^4 \rangle$ is the increasing localization of the d electrons of the conduction band at the non-rare earth ion on the transition from Rh to Zn and the absence of d electrons in Mg. The sign of the calculated $A_4\langle r^4 \rangle$ is obtained incorrectly, so that it is necessary to assume an additional contribution of the same order but opposite sign, for example, anisotropic exchange between the $4f$ electrons and the conduction-band electrons. The observed values for $A_6\langle r^6 \rangle$ are not reproduced by these calculations. This is usually attributed to the circumstance that covalent effects play a large part and the conduction electrons near the rare-earth ion have a weak f nature.³⁷

Neutron-scattering experiments have also been made on isostructural compounds of the light rare-earth ions Pr and Nd with a view to determining the crystal-field parameters, but these experiments could not be unambiguously described by a single set of crystal-field parameters.³⁵ Here, the data are not yet so complete as for the holmium and erbium compounds.

Structure of $MgCu_2(C15)$ type. The cubic structure of the Laves phase of $MgCu_2(C15)$ type is the largest family of isostructural rare-earth compounds. The existence of rare-earth M_2 compounds has been proved for almost all rare-earth atoms with $M = Mg, Al, Mn, Fe, Co, Ni, Ru, Rh, Pd, Os, Ir$.^{9,41} However, systematic study

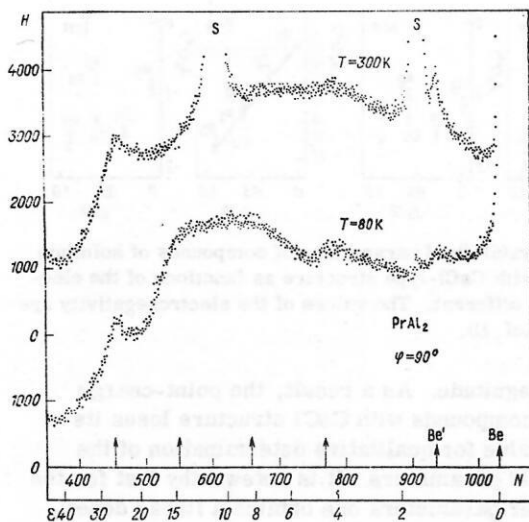


FIG. 11. Spectrum of neutron scattering by PrAl_2 .⁴⁶ Because of the large widths of the lines of the transitions between the crystal levels, the spectrum exhibits little structure.

of the crystal field by means of inelastic neutron scattering has hitherto been restricted to the rare-earth compounds with Al_2 . Therefore, we shall restrict ourselves here to this series of compounds. They all exhibit magnetic order, and therefore a number of neutron-scattering experiments were made on dilute samples.⁴²⁻⁴⁴ In the experiments on concentrated compounds, one observes large line widths of the transitions due to the crystal field, which complicates the unambiguous determination of the crystal-field parameters (Fig. 11).^{45,46} The crystal-field parameters were also determined from investigations of magnetic elementary excitations by means of inelastic neutron scattering by single crystals⁴⁷⁻⁴⁹ and experiments on the magnetization of single crystals.^{50,51}

If one uses the experimentally obtained crystal-field parameters to calculate B_4^0 , B_6^0 and A_4 , A_6 , using the relativistic radial integrals $\langle r^n \rangle$,¹³ the result shown in Fig. 12 (Ref. 51) is obtained. The crystal-field parameters hardly depend on the rare-earth ion through the rare-earth Al_2 series, so that the parameters satisfy the simple relation

$$B_4^0 \sim \langle r^4 \rangle \beta_J a^{-5}; \quad B_6^0 \sim \langle r^6 \rangle \gamma_J a^{-7}, \quad (23)$$

where β_J and γ_J are numerical factors (see Ref. 12). This result can be explained as follows: Either the contribution of the conduction electrons to the potential of the crystal field is small, or their influence through the

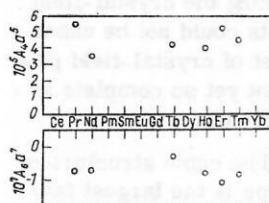


FIG. 12. Reduced crystal-field parameters $A_\alpha a^{-(\alpha+1)}$ for compounds of rare-earth elements with Al_2 obtained from the experimental values of Be^m using the relativistic radial integrals $\langle r^\alpha \rangle$.¹³

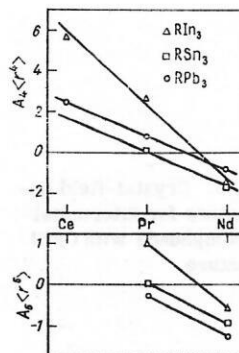


FIG. 13. Change in the crystal-field parameters for Cu_3Au structure with different ions of the rare-earth element.⁵³

rare-earth series does not change.⁵¹ The constancy of $A_6 a^7$ indicates that in this group of compounds, in contrast to the case considered above, the sixth-order parameters also satisfy a certain systematic relationship.

The crystal-field parameters found in Ref. 45 for HoAl_2 and TmAl_2 do not fit into this picture. True, only one or two inelastic peaks were observed in the neutron-scattering experiments, so that the interpretation could be uncertain. As yet, there are no results of investigations of the crystal field by inelastic neutron scattering in compounds with other partners. Experiments on PrNi_2 reveal values of the crystal-field parameters close to those for PrAl_2 .⁵²

Structure of $\text{Cu}_3\text{Au}(\text{L}1_2)$ type. In a cubic crystal structure of Cu_3Au type, investigations of the crystal field by inelastic neutron scattering and measurement of the susceptibility have hitherto been made principally for REEX_3 systems, where REE are the light rare-earth elements Ce, Pr, and Nd, and X represents Pd, In, Sn, Tl, and Pb.⁵³⁻⁵⁶ The compound Pr_3Tl also crystallizes in this structure, and it has become a model material for investigating the dynamics of the so-called singlet-triplet systems and will be considered in the following subsection in somewhat more detail. In Ref. 53, rare-earth-element compounds were studied ($\text{REE} = \text{Ce, Pr, Nd}$; $\text{X} = \text{In, Pb, Sn}$). It was established for the crystal-field parameters that with increasing number of 4f electrons their value decreases and, in addition, there is a change of sign (Fig. 13). Such behavior can be explained by delocalization of the 4f electrons at the beginning of the rare-earth series⁵³ or by a change in the contribution of the exchange interaction to the crystal field.⁵⁷ For the isoelectron rare-earth compounds with Sn_3 and Pb_3 the parameters $A_4 \langle r^4 \rangle$ and $A_6 \langle r^6 \rangle$ have the same dependence on the rare-earth ion, whereas for the rare-earth compounds with In_3 the dependence is stronger. This could be regarded as an indirect proof of influence of the conduction electrons.

The crystal-field parameters obtained from neutron experiments on isostructural compounds of rare-earth elements with Pd_3 in Ref. 54 also revealed no changes. For them, the $A_4 \langle r^4 \rangle$ values were found to be negative and almost equal to each other within the experimental errors; the parameters $A_6 \langle r^6 \rangle$ have positive values.

Investigations of compounds in the series PrX_3 (X

= In, Tl, Sn, Sb) by inelastic neutron scattering⁵⁵ gave crystal-field parameters in which the $A_4\langle r^4 \rangle$ values exhibit a systematic variation. With increasing difference between the electronegativities, the values of $A_4\langle r^4 \rangle$ decrease. The value of $A_4\langle r^4 \rangle$ for PrPd₃ found in Ref. 54 also does not contradict this tendency, but it is nevertheless impossible to construct a linear dependence, since the absolute value for PrPd₃ is clearly too low. For the parameters $A_6\langle r^6 \rangle$ a systematic variation was not found.

2.2. Investigation of the crystal field in rare-earth intermetallic compounds with hexagonal crystal structure

Hitherto, very few experiments have been made using neutron scattering by intermetallic compounds with hexagonal crystal structure. There are some data on rare-earth compounds with Al₃ (the rare earths Ce, Pr, and Nd) with Ni₃Sn structure.⁵⁸⁻⁶¹ The spectra of these compounds reveal well-resolved peaks, which can be ascribed to transitions between crystal levels. Figure 14 shows the inelastic neutron-scattering spectrum for PrAl₃.^{58,60} The obtained crystal-field parameters show that the terms of second, fourth, and sixth order participate to about the same extent in the formation of the crystal field. In the interpretation of the measurements of the susceptibility and specific heat in hexagonal compounds, the contribution of second order to the crystal field is ignored for simplicity. Since one then obtains a satisfactory explanation of the measured quantities, it appears that this term can be ignored.

The interpretation of the spectra of the scattered neutrons is more difficult than in the case of a cubic crystal field, since for hexagonal symmetry there are four independent parameters of the crystal field (see Sec. 1). To reduce the number of independent parameters, one introduces the ratio $V = B_6^6/B_6^0$, which is usually calculated in the point-charge model. The approximation for determining this quantity on the basis of the ideal c/a ratio of the hexagonal lattice gives $V = 77/8$ and is insufficiently good. For PrAl₃ with a value of V calculated using the real lattice parameters one obtains better agreement with the experiment than with $V = 77/8$.⁶⁰ Our investigations with PrNi₅ (CaCu₅-type

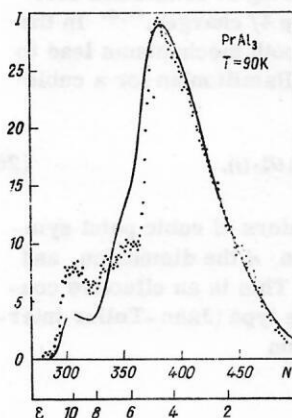


FIG. 14. Spectrum of neutron scattering associated with transitions between the crystal-field levels of the hexagonal compound PrAl₃.⁶⁰

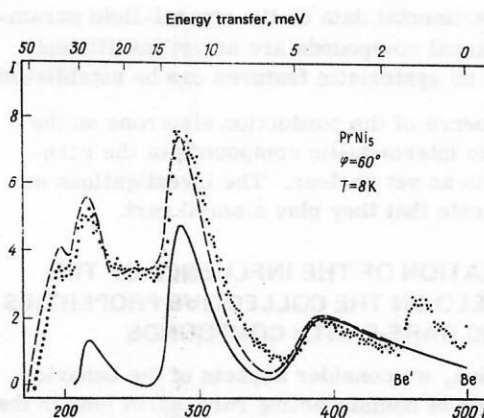


FIG. 15. Spectrum of neutron scattering associated with the transitions between the crystal-field levels of the hexagonal compound PrNi₅.⁶²

structure) show that by changing V one can improve the agreement between the experimentally measured spectrum and the calculated spectrum⁶² (Fig. 15).

For the intermetallic compounds with hexagonal symmetry there are as yet too few results for general conclusions to be drawn. Investigations with this group of substances could in the future become a fruitful direction in investigations by neutron scattering, since, on the one hand, the experimental technique has now been sufficiently developed and, on the other, the neutron-scattering spectra may contain richer information because of the large number of possible transitions between the crystal levels in the hexagonal crystal field.

2.3. Conclusions

The above results of the study of the crystal field in rare-earth compounds permits the following conclusions to be drawn.

1. In the rare-earth compounds with NaCl structure (pnictides and chalcogenides) the fourth-order term makes a significant contribution to the crystal field. In the intermetallic compounds with other types of cubic structure, the contributions from $A_6\langle r^6 \rangle$ are of the same order of magnitude as the $A_4\langle r^4 \rangle$ contributions. When the metallic nature of the substances is more clearly expressed, the contribution to the crystal potential of the sixth-order terms is greater.

2. The fourth-order parameters in the various groups of compounds exhibit certain systematic tendencies, whereas this is not found for the sixth-order parameters.

3. Attempts at qualitative (linear dependence of the crystal-field parameters on the difference between the electronegativities) and quantitative (calculations of the band structure for CsCl structure) explanation of the crystal-field parameters have been successful only for the $A_4\langle r^4 \rangle$.

4. The model of effective point charges gives good agreement with the experiments only for monpnictides and monochalcogenides of the rare-earth elements. It fails for the intermetallic compounds.

5. The experimental data on the crystal-field parameters in hexagonal compounds are as yet insufficient, and therefore no systematic features can be established.

6. The influence of the conduction electrons on the crystal field in intermetallic compounds of the rare-earth metals is as yet unclear. The investigations so far made indicate that they play a small part.

3. INVESTIGATION OF THE INFLUENCE OF THE CRYSTAL FIELD ON THE COLLECTIVE PROPERTIES OF METALLIC RARE-EARTH COMPOUNDS

In this section, we consider aspects of the behavior of the ensemble of noninteracting rare-earth ions in the effective environment (point charges + conduction electrons + chemical bond), in particular the effects due to the exchange interaction between the rare-earth ions in the lattice, which may lead to an ordered state at low temperatures. Inelastic neutron scattering is in its kind a unique method for studying collective excitations in a condensed medium. Because of the two principal types of interaction of thermal neutrons with matter, one can relatively easily observe phonons and magnetic excitations, but it is difficult to excite electron quadrupole transitions between different crystal levels. It follows from this that for the study of magnetic excitations (spin waves) inelastic neutron scattering is the principal method of investigation, whereas in the investigation of structural phase transitions of the Jahn-Teller type (quadrupole coupling) inelastic neutron scattering is restricted to the determination of the splitting (the level scheme) of the rare-earth ions in the crystal field.

In metallic compounds of rare-earth elements there are a number of interaction mechanisms which lead to an effective exchange coupling of the rare-earth ions at different sites of the crystal lattice. Because of the strong localization of the $4f$ electrons ($\langle r_{4f}^2 \rangle^{1/2} \approx 0.45 \text{ \AA}$), they interact not directly, but indirectly through the system of conduction electrons or the system of phonons. The form and strength of these interactions determine the cooperative behavior of the metallic compounds of the rare-earth elements. The following interaction mechanisms can be identified.

a) An isotropic magnetic dipole-dipole interaction is realized indirectly through the conduction electrons. It determines the magnetic behavior of metallic systems of the rare-earth elements. Many compounds of rare-earth elements have magnetic phase transitions at temperatures below 100°K . The $4f$ electrons (with spin S) give rise to a long-range oscillating spin density of the conduction electrons (with spin s), which leads to a coupling of the rare-earth ions at different lattice sites. The Hamiltonian of the interaction of the $4f$ electrons with the conduction electrons is

$$H_{sf} = -\Gamma_{sf} S \cdot s, \quad (24)$$

where Γ_{sf} is the sf exchange integral. In the description of the coupling of two rare-earth ions at the lattice sites i and j in the model of effective ff exchange interaction (without explicit allowance for the lattice system and the correlation of the conduction electrons), one

obtains an isotropic Heisenberg exchange interaction of the spins of the form

$$H_{\text{exch}} = -\frac{1}{2} \sum_{i,j} I_{ij} J(i) J(j). \quad (25)$$

Because of the strong spin-orbit interaction, the total angular momentum J is a good quantum number. The indirect magnetic exchange coupling through the conduction electrons of the Ruderman-Kittel-Kasuya-Yosida (RKKY) type⁶³ depends on the electron density in the conduction band.⁶⁴

Of particular experimental and theoretical interest is the investigation into the nature of induced magnetic phase transitions. Such phase transitions are usually observed in systems with a nonmagnetic ground state. Typical representatives are PrAl_2 (Ref. 46) and Pr_3Ti (Ref. 65), which will be considered in detail later. For systems with a singlet ground state, the condition for the onset of magnetic instability in the molecular-field approximation is⁷¹

$$h_m = 4I(0) \alpha^2 / \Delta > 1,$$

where $\alpha = \langle 0 | J_z | 1 \rangle$, J_z are the matrix elements between the ground state $|0\rangle$ and the first excited state $|1\rangle$, Δ is the corresponding energy difference, and $I(0) (q=0)$ is the Fourier component of the ferromagnetic exchange integral. Thus, the magnetic exchange must reach a critical value relative to the effect of the crystal field if long-range magnetic ordering is to occur.

b) Quadrupole coupling of the rare-earth ions is realized through the phonon system and quadrupole scattering of the conduction electrons by the system of $4f$ charges. A number of metallic and nonmetallic rare-earth compounds have been studied by measurements of the velocity of sound. A strong temperature dependence of the elastic constants was observed, these becoming softer near the phase-transition point. One can also observe structural phase transitions, expressed in a distortion of the lattice.

In this case, one speaks of a cooperative Jahn-Teller phase transition.⁶⁶ The anomalies of the elastic properties can be satisfactorily described by means of coupling of phonons to ions subject to the influence of the crystal field but not interacting with one another,^{67,68} and also by quadrupole scattering of conduction electrons by the distribution of the $4f$ charges.^{67,69} In the effective-interaction model, both mechanisms lead to an ion-ion interaction whose Hamiltonian for a cubic lattice has the form

$$H_{\text{int}}^{\text{JT}} = -\frac{1}{2} \sum_{i,j} K_{ij}(\alpha d) O_{\alpha d}^n(i) O_{\alpha d}^n(j), \quad (26)$$

where $O_{\alpha d}^n(i)$ are tensor operators of cubic point symmetry (α is the representation, d the dimension, and n the degree of degeneracy). This is an effective coupling of the ions of quadrupole type (Jahn-Teller interaction), and under the condition

$$h_e = 4K(0) \beta^2 / \Delta > 1$$

it leads to an induced structural instability; β are the corresponding matrix elements of the quadrupole operators, and $K(0)$ describes the $q=0$ Fourier compo-

TABLE II. Characteristic examples of metallic compounds of rare-earth elements with magnetic and structural phase transitions investigated by means of inelastic neutron scattering.

Phase transition	Substance	Investigated characteristics
Magnetic, $h_m > 1$	PrAl ₂ , Pr ₃ Tl, TbSb	Dispersion and temperature dependence of magnetic elementary excitations
	NdAl ₂ , NdSb, TbAl ₂ , HoZn, HoP, HoFe ₂ , ErFe ₂ , Ho _{0.88} Tb _{0.12} Fe ₂ PrSb (under the influence of pressure)	Dispersion of magnetic elementary excitations at constant temperature
Structural, $h_e > 1$	PrCu ₂ , TmCd Dielectrics: PrAlO ₃ , TmVO ₄ , DyVO ₄ , TbVO ₄	Velocity of sound; coupled excitation-phonon spectrum; magnetic excitations
Magnetic + structural at the same temperature, h_m or $h_e > 1$ and $h_{me} > 1$	TbP, TbAs, TbSb, DySb, HoSb, TbZn, DyZn, TbCu	Excitation of crystal levels in the paramagnetic phase
Magnetic + structural at different temperatures	Pr ₃ Se, TmZn	Excitation of crystal levels in the paramagnetic phase

ment of the quadrupole interaction K_{ij} .

c) A coupling can be established between the system of phonons and the magnetically interacting system. In this case, one obtains a bound spectrum of phonons and magnetic excitations, which under certain symmetry conditions may not intersect and may even repel one another.⁶⁷⁻⁷⁰ If the coupling of the two systems is sufficiently strong ($h_m > 1$ and $h_{me} > 1$ or $h_e > 1$), then magnetic and structural phase transitions may occur at the same temperature.⁷¹ Characteristic examples of metallic compounds of rare-earth elements in which the above phase transitions occur at the same or different temperatures, and also compounds in which the spectrum of elementary excitations has been investigated by inelastic neutron scattering are given in Table II.

d) One can also have multipole interactions of higher order, which can lead to phase transitions⁷² of higher polarity. Since they have not yet been observed experimentally, we shall limit the following considerations to the three listed interaction mechanisms.

3.1. Systems with magnetic phase transition

There are various experimental possibilities for studying magnetic phase transitions (measurement of the specific heat, magnetization, susceptibility, electrical conductivity, and so forth). However, only inelastic neutron scattering enables one to study directly the dynamics of the spins of magnetic crystals and, therefore, the microscopic nature of the phase transition. For this, investigations into the temperature dependence of the spectra of magnetic excitations have been made in the last ten years by means of inelastic neutron scattering for a number of rare-earth elements and their compounds.

Magnetic phase transitions of the second kind, which occur in this group of substances, are characterized by the presence of a singularity in the static magnetic sus-

ceptibility. This singularity may be caused by a softening of a branch of elementary excitations or by the manifestation of a so-called central mode ($\omega=0$) of the corresponding symmetry.⁶⁵ To describe this effect, one usually employs the following expression for the neutron scattering cross section:

$$\frac{d^2\sigma}{d\Omega d\omega} = \frac{A}{[1 - \exp(-\omega/kT)]} \sum_{\alpha, \beta} \left(\delta_{\alpha\beta} - \frac{\kappa_\alpha \kappa_\beta}{\kappa^2} \right) \times \text{Im } \chi_{\alpha\beta}(\mathbf{q}, \omega), \quad \beta\alpha = +, -, z, \quad (27)$$

where A is a constant; κ and ω are the momentum and energy transfers of the neutrons, and $\mathbf{q} = \kappa - \tau$ (τ is a vector of the reciprocal lattice). The factor $\delta_{\alpha\beta} - \kappa_\alpha \kappa_\beta / \kappa^2$ makes it possible to distinguish longitudinal and transverse excitations. The poles of the magnetic susceptibility $\chi_{\alpha\alpha}(\mathbf{q}, \omega)$ and $\chi_{zz}(\mathbf{q}, \omega)$ determine the transverse and longitudinal excitations, respectively. The residue of the susceptibility at the poles determines the intensity of the peaks in the inelastic neutron-scattering spectrum. In the molecular-field-random-phase approximation, the poles of the dynamic susceptibility are δ functions in ω . By taking into account scattering processes of higher order (with conduction electrons or phonons) one can explain the lifetimes and, thus, the widths of the peaks.

3.1.1. Investigation into the nature of magnetic phase transitions. For metallic compounds of rare-earth elements, there exist some model substances with nonmagnetic ground state in which the magnetic exchange exceeds the critical value $h_m > 1$, so that at low temperatures a magnetic phase transition occurs. Because of the magnetic exchange, the wave functions of the excited magnetic states are mixed to the nonmagnetic ground state and induce in it a magnetic moment.

The most detailed investigations of the temperature dependence of the spectra of elementary excitations near a phase transition have been made for cubic single crystals (or polycrystals) of PrAl₂,⁴⁹ Pr₃Tl,⁶⁵ and TbSb,⁷³ which we shall now consider.

1. PrAl₂. This is the only compound so far discovered in which the ground state is a nonmagnetic doublet. It orders ferromagnetically ($T_C = 32^\circ\text{K}$, $h_m \approx 1.3$), and the saturation moment at $T=0$ in the direction of easy magnetization (the z axis) is 80% of the moment of the free ion. The $3H_4$ ground multiplet is split in a cubic field into $\Gamma_3(0)$, $\Gamma_4(\Delta)$, $\Gamma_1[(12/5)\Delta]$, and $\Gamma_6(\Delta')$ with $\Delta = 2.36$ meV and $\Delta' = 13.7$ meV.⁷⁴ The magnetic elementary excitations were investigated by means of inelastic neutron scattering.⁴⁹ Figure 16 shows the PrAl₂ dispersion curves for excitations along the directions $[0, 0, \xi]$ and $[\xi, \xi, 0]$. They exhibit relatively weak dispersion. At $\xi=0.5$ in the direction $[0, 0, \xi]$ interaction of a longitudinal acoustic phonon with low-lying magnetic excitations is manifested. The broken curve is the dispersion curve of the acoustic phonon at $T=300^\circ\text{K}$. Such an interaction can also be assumed near $\xi=0.4$ in the direction $[\xi, \xi, 0]$. Such an effect of the phonons on the magnetic excitations is obtained as a result of coupling of the acoustic phonons to the magnetically interacting system. In these regions, there is apparently repulsion of the two kinds of excitation.^{70, 75}

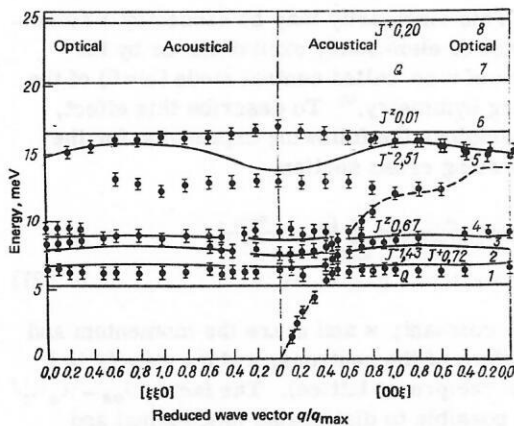


FIG. 16. Dispersion curves of spin waves in PrAl_2 in the directions $[00\xi]$ and $[\xi\xi0]$.⁷⁸

For the most intense transverse magnetic branch (at energy ≈ 15 meV) with the strongest dispersion one observes a splitting that obviously reduces to two independent groups of excitations for J_x and J_y , the splitting being due to the strong anisotropic exchange interaction.⁷⁶ In addition, in the experiments with PrAl_2 measurements at higher temperature revealed spin waves derived from excited states (Fig. 17), which were observed for the first time in TbAl_2 .⁷⁷ Investigation of the temperature dependence of the magnetic excitations near $q=0$ revealed a partial softening of their energy, though this did not reach zero at the phase transition. Experiments with higher resolution showed that the principal part of the magnetic scattering near $T \rightarrow T_{\text{cr}}$ is elastic (Fig. 18).⁷⁸ This is an experimental indication of a central peak $\omega=0$, whose intensity increases at the phase transition because of the critical fluctuations.

2. TbSb . This is an antiferromagnet with singlet ground state ($T_N = 14.9^\circ\text{K}$, $h_m = 3.5$). The first excited level is a triplet at $\Delta = 1.2$ meV. For this compound, the spin-wave spectrum near $q=0$ has also been investigated in detail⁷³ and behavior analogous to PrAl_2 has been found. As the phase-transition point is approached, $T \rightarrow T_N$, the frequencies of the elementary excitations decrease but remain nonzero at $T = T_N$. Also observed is a central peak ($\omega=0$), whose intensity increases (Fig. 19) as the transition point is approached.

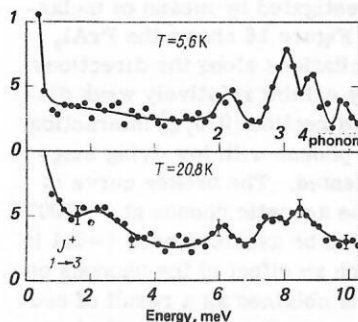


FIG. 17. Temperature dependence of neutron scattering by PrAl_2 for $q = (2\pi/a) [2, 2, 0.7]$. The peak at energy ≈ 2 MeV ($T = 20.8^\circ\text{K}$) is a transition between the I and III excited states.⁸

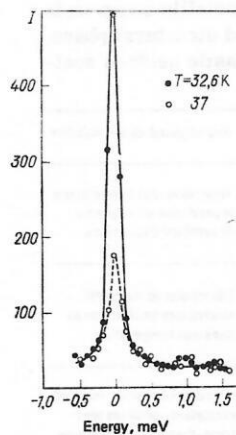


FIG. 18. Temperature dependence of neutron scattering by PrAl_2 near T_{cr} (above T_{cr}) for $q = [2.06, 2.06, 0]$.⁷⁸

3. Pr_3Tl . This, the most intensively investigated material, is a clear example of a critical ferromagnet ($h_m = 1.014$) with a singlet ground state ($T_C = 11.5^\circ\text{K}$). The saturation moment at $T=0$ is $\sim 20\%$ of the moment of the free ion. In the crystal field, the ground-state multiplet is split into $\Gamma_1(0)$, $\Gamma_4(\Delta)$, $\Gamma_3[(12/7)\Delta]$, $\Gamma_5(\Delta')$ with $\Delta = 4.5$ meV and $\Delta' = 16$ meV.⁷⁹ Inelastic neutron-scattering experiments at momentum transfer $q = 0.6 \text{ \AA}^{-1}$ reveal an almost temperature-independent position of the magnetic excitation (Fig. 20). This can be explained only by taking into account in the calculations the entire level scheme.⁸³ The experimental realization of the case $q \rightarrow 0$, for which a stronger temperature dependence is expected (softening at the phase transition), was thwarted by admixture of the direct neutron beam. Nevertheless, it is to be expected that the $\Gamma_1 - \Gamma_4$ branch becomes completely soft near the phase transition. Critical $\omega=0$ scattering, as in PrAl_2 and TbSb , is also observed in Pr_3Tl , its intensity increasing strongly at T_C (Fig. 21).⁸⁰ Although the critical ratios of the exchange to the splitting by the crystal field h_m for Pr_3Tl and TbSb differ (1:3), it is expected that the phase transition is described by the same mechanism.

3.1.2. Investigation of spin waves. Here, we con-

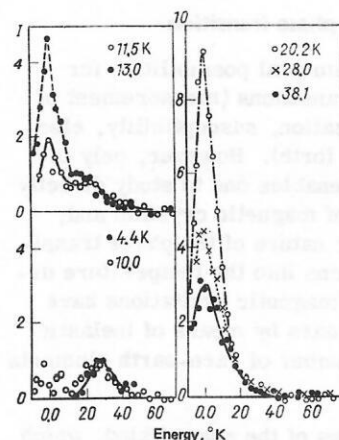


FIG. 19. Temperature dependence of spin waves and the central peak in TbSb for $q = [0.05, 0.05, 0.05]2\pi/a$.⁷³

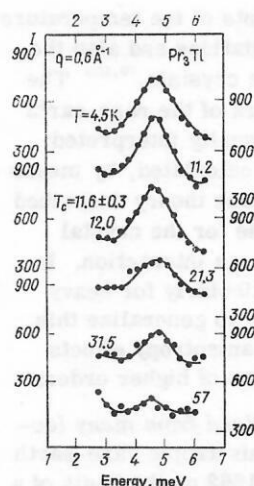


FIG. 20. Temperature dependence of neutron scattering by Pr_3Tl at $q = 0.6 \text{ \AA}^{-1}$.⁸⁴

sider the results of investigations of the dispersion of spin waves at constant temperature in materials with cubic and hexagonal structure.

Cubic structure. 1. NdAl_2 . The ground state is a Kramers doublet and ferromagnetic ordering occurs at $T_C = 77.2^\circ\text{K}$. The energies of the splitting by the crystal field and the exchange energy in NdAl_2 are comparable in magnitude. The saturation moment at $T=0$ is 76% of the moment of the free ion Nd^{3+} . Investigations of the dispersion of the spin waves by means of inelastic neutron scattering⁹² reveal the existence of three independent groups of excitations for J_+ , J_- , and J_z . Figure 22 shows the dispersion relations for NdAl_2 at $T=4.2^\circ\text{K}$ for wave vector in the direction $\langle 001 \rangle$. Since there are two magnetic atoms per unit cell in NdAl_2 , acoustical and optical branches are observed for all operators J_α ($\alpha = +, -, z$). In addition, near the center of the band a fourth optical excitation is observed. At the edge of the band, the optical and acoustical excitations are degenerate. A fairly good description of the experimental dispersion curves (the continuous curves in Fig. 22) is obtained by means of the theory of pseudobosons.¹¹ The exchange-interaction parameter obtained from the analysis of the experiment reveals RKKY behavior (Fig. 23).

2. TbAl_2 . The ground state is a singlet, and the first excited level a triplet. The strong exchange interaction leads to ferromagnetic ordering at $T_C = 105^\circ\text{K}$. The saturation moment at $T=0$ is ~89% of the moment of the free Tb^{3+} ion. The magnetic excitations in the ordered phase are spin waves with an energy gap at the center of the band. It is due to the anisotropy of the crystal. The spectrum of magnetic excitations can be described by means of the formalism presented in Sec. 3.1.3. An interaction was observed for the first time in this material between excitations derived from the ground state and from excited states.⁷⁷ The effect can be explained

¹¹At $T=0$, the pseudoboson theory is equivalent to the theory of spin waves derived from many levels presented in Sec. 3.1.3. It is not valid at temperatures of the order of the splitting by the crystal field.

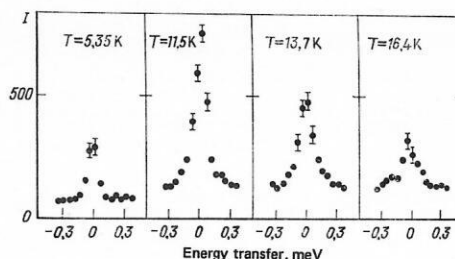


FIG. 21. Temperature dependence of the intensity of the central peak in Pr_3Tl at $q = 0.06 \text{ \AA}^{-1}$.⁸⁰

by taking into account the complete level scheme in the theoretical explanation.⁸⁶ The effect was also observed later in PrAl_2 (see Sec. 3.1.1).

3. HoZn . This orders ferromagnetically at $T_C = 75^\circ\text{K}$ and is a triplet-doublet system. The spectrum of spin waves has been investigated at $T=4.2^\circ\text{K}$,⁹³ and measurements made of two branches along principal symmetry directions. The results were analyzed by means of the Green's-function method (see Sec. 3.1.3), and the dispersion curves were reproduced, the biquadratic exchange terms in the Hamiltonian operator being taken into account.

4. HoP . The ground state is a doublet, the first excited level a triplet, and ferromagnetic ordering occurs at $T_C = 5.5^\circ\text{K}$. Inelastic neutron-scattering measurements were made at $T=1.5^\circ\text{K}$ of five spin-wave branches, whose energy positions are almost independent of the wave vector.⁹⁴ The results were described by including bilinear and quadrupole interactions in the effective single-ion Hamiltonian. At $T=4.2^\circ\text{K}$, a spin wave deriving from an excited state was observed.

5. Rare-earth-transition-metal compounds are of particular interest because of technological applications as permanent magnets and hydrogen absorbents. Measurements of the spin waves in these systems were made with a view to studying the exchange interactions and also the crystal field and magnetoelastic properties in, for example, polycrystalline samples of ErFe_2 and HoFe_2 (Ref. 95) and single crystals of ErFe_2 (Ref. 96), $\text{Ho}_{0.88}\text{Tb}_{0.12}\text{Fe}_2$ (Ref. 97), and HoFe_2 (Ref. 98). In these compounds, the magnetism is determined by the Fe-Fe

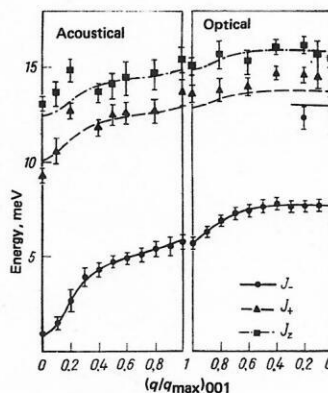


FIG. 22. Dispersion curves of magnons in NdAl_2 at $T=4.2^\circ\text{K}$ for wave vector along $\langle 001 \rangle$. The continuous curves are calculated in accordance with the pseudoboson model.⁹²

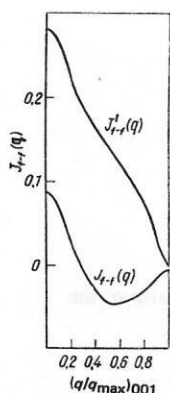


FIG. 23. Exchange interaction parameters J_{f-f} and J'_{f-f} for NdAl_2 at $T = 4.2^\circ\text{K}$ in the direction $\langle 001 \rangle$.⁹²

or Fe-rare-earth interaction, which is much stronger than the rare-earth-rare-earth interaction. All these substances order magnetically at a temperature much higher than room temperature. As an example, Fig. 24 shows the dispersion curves of the first three low-lying spin-wave branches for HoFe_2 (Ref. 98) in the direction $[110]$ at room temperature and at $T = 10^\circ\text{K}$. Altogether, six spin waves are expected; the three branches absent in the figure lie above 200 meV and could not be observed by means of the inelastic scattering of thermal neutrons. A good theoretical description of these experiments is obtained by means of the theory of spin waves derived from many levels (see Sec. 3.1.3) when allowance is made for the crystal field and also isotropic exchange interaction of nearest neighbors (continuous curves in Fig. 24).

Inelastic neutron scattering was also used to investigate spin waves in NdSb ,¹⁰¹ ErCu ,¹⁰² and PrSb ,¹⁰³ which were investigated under pressure.

Hexagonal structure. For hexagonal structures of metallic compounds of rare-earth metals spin-wave investigations have not yet been made, and only the rare-earth metals themselves have been investigated. Whereas the spin-wave spectra have been investigated rather fully^{76,99} for heavy rare-earth metals by means of inelastic neutron scattering, for the light rare-earth

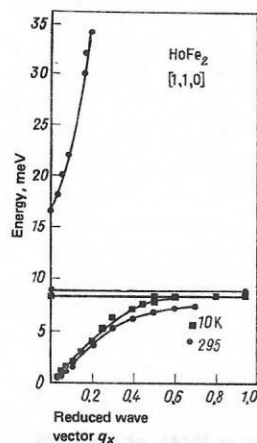


FIG. 24. Dispersion of magnons in HoFe_2 at $T = 300$ and 10°K in the direction $\langle 110 \rangle$.

metals there are only measurements of the temperature dependence of the elementary excitations and also the dispersion in Pr and Pr-Nd single crystals.^{76,100} The inelastic neutron-scattering spectra of the rare-earth metals and their compounds are usually interpreted, and their macroscopic properties calculated, by means of the molecular-field-random-phase theory described in Sec. 3.1.3, allowance being made for the crystal field and isotropic magnetic exchange interaction. In the case of some compounds, particularly for heavy rare-earth metals, it is necessary to generalize this Hamiltonian and take into account anisotropy effects and also magnetoelastic interactions of higher orders.

3.1.3. Theory of spin waves derived from many levels. A theory of spin waves for anisotropic rare-earth systems was developed⁸¹ in 1960–1962 on the basis of a Holstein–Primakoff transformation.⁸² With the accumulation of experimental information on systems in which an influence of the crystal field is manifested, it became necessary to develop a theory that takes into account as accurately as possible the crystal field. This led to the development of the pseudospin and pseudoboson theories for systems with crystal field,⁸³ but these are valid only at $T = 0$ and thus admit excitations deriving from only the ground state. Spin waves deriving from excited states such as are observed in, for example, PrAl_2 and TbAl_2 , and their influence on the complete excitation spectrum at a temperature $T \sim \Delta/k$, as, for example, the interaction of two branches in $(\text{Pr}_{0.88}\text{La}_{0.12})_3$,⁸⁴ cannot be described in the framework of pseudoboson theory. The influence of branches that derive from excited states is also completely ignored in models like the singlet-singlet and singlet-triplet models. These models predict strongly temperature-dependent excitation bands that are not in reality observed (Pr_3Tl , PrAl_2 , TbSb). In 1971–1972, various authors^{85,86} generalized these theories independently of one another. They showed that when allowance is made for all levels of the ground-state multiplet one can obtain comparatively simple expressions for the spectrum of magnetic elementary excitations by means of the combined molecular-field-random-phase theory for the magnetic susceptibility $\chi_{\alpha\beta}(\mathbf{q}, \omega)$. This comparatively simple method of theoretical description, which gives good agreement with the experimental data, will be described here briefly with a view to subsequent discussion of the experimental results.

Under the assumption that in the substances discussed above the effects of anisotropy in magnetic exchange, multipolarities of higher order, and the influence of the phonons on the magnetic system play a secondary role (PrAl_2 is an exception), the point of departure for the theoretical description of the spectrum of elementary excitations is the isotropic Hamiltonian

$$H = H_{\text{mf}} + H_{\text{exch}} \quad (28)$$

Here, the Hamiltonian H_{mf} includes the crystal field and the molecular field and is a single-ion Hamiltonian operator,

$$H_{\text{mf}} = H_{\text{cf}} - h \sum_i J(i), \quad (29)$$

where $h = I(0)\langle J \rangle$ is the molecular field, and H_{exch} , in

contrast to the expression (25), is the pure two-ion contribution:

$$H_{\text{exch}} = -\frac{1}{2} \sum_{i,j} I_{ij} \delta \mathbf{J}(i) \delta \mathbf{J}(j);$$

$$\delta \mathbf{J}(i) = \mathbf{J}(i) - \langle \mathbf{J}(i) \rangle. \quad (30)$$

By diagonalizing H_{mf} one calculates the order parameter $\langle \mathbf{J} \rangle$, the single-ion energies ω_n , and the wave functions of the states $|n\rangle$ by means of the following relation for the self-consistent molecular-field approximation for

$$\langle \mathbf{J} \rangle = \sum_n \langle n | \mathbf{J} | n \rangle \exp(-\omega_n/kT) / \sum_n \exp(-\omega_n/kT). \quad (31)$$

To study the dynamics of the spin system, it is necessary to calculate the dependence of the elementary excitations on q (which extends the molecular-field model). For this, one introduces the following Green's function⁸⁷:

$$G_{\alpha\beta}(ij, t) = i\theta(t) \langle [\delta J_{\alpha}(i, t), \delta J_{\beta}(j, 0)] \rangle. \quad (32)$$

To describe the single-ion states,⁸⁷ the creation and annihilation operators $c_n^*(i)$ and $c_n(i)$ are introduced; then the diagonal representation of the single-ion Hamiltonian of the molecular field has the form

$$H_{\text{mf}} = \sum_{i,n} \omega_n c_n^*(i) c_n(i). \quad (33)$$

The spin operators in Eq. (30) can be expanded with respect to the basis of single-ion states:

$$\mathbf{J}(i) = \sum_{n,m} \langle m | \mathbf{J}(i) | n \rangle c_m^*(i) c_n(i). \quad (34)$$

Fermi commutation relations hold for the creation and annihilation operators. The description of thermodynamic properties such as, for example, the order parameter by means of c -number operators is valid only in the self-consistent molecular-field approximation.⁸⁸ In a higher self-consistent approximation of the random-phase type it is physically unjustified to treat the thermodynamics of the system in the framework of such notions, since the single-ion states do not possess simple Fermi statistics.

For the dynamic susceptibility in the non-self-consistent molecular-field-random-phase approximation we obtain

$$\chi_{zz}(\mathbf{q}, \omega) = \frac{g_{zz}(\omega)}{1 + I(\mathbf{q}) g_{zz}(\omega)}; \quad \chi_{+-}(\mathbf{q}, \omega) = \frac{g_{+-}(\omega)}{1 + (1/2) I(\mathbf{q}) g_{+-}(\omega)}, \quad (35)$$

with the single-ion susceptibility

$$g_{\alpha\beta}(\omega) = \sum_{m,n} \frac{2J+1}{\omega - \omega_n + i\omega_m} \frac{\langle m | J_{\alpha} | n \rangle \langle n | J_{\beta} | m \rangle (f_m - f_n)}{\omega - \omega_n + i\omega_m} \quad (36)$$

(f_n are the populations of the energy levels).

The self-consistent extension of the random-phase approximation for determination of the order parameter by means of sum rules for the spin quantities leads to an unphysical allowance for fluctuations.⁸⁸ The non-self-consistent molecular-field-random-phase theory is at the present time a good and simple method for analyzing and interpreting inelastic neutron-scattering experiments.

By means of Eqs. (35) it was possible to explain the spectrum of magnetic excitations of Pr_3Tl and TbSb .^{65,67} Figure 25 shows the calculated magnetic excitations in Pr_3Tl as functions of the temperature for

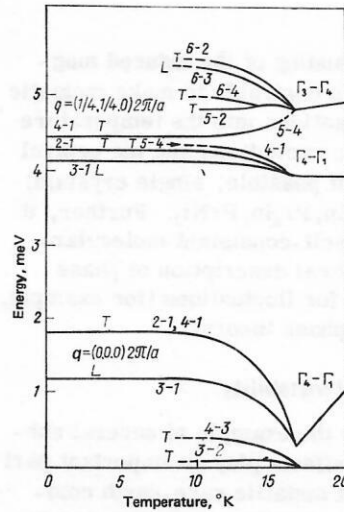


FIG. 25. Temperature dependence of magnetic excitations in the ferromagnetic phase of Pr_3Tl ($T_c = 11.6^\circ\text{K}$) for the center of the band $q = (0, 0, 0)2\pi/a$ and for $q = (1/4, 1/4, 0)2\pi/a$ (L and T stand for longitudinal and transverse).

the center of the band, $q = (0, 0, 0)2\pi/a$, and for $q = (1/4, 1/4, 0)2\pi/a$. The excitations for $q = 0$ (the experimental realization is very difficult) exhibit a strong temperature dependence. In contrast, the excitations in the case of finite values of q depend much more weakly on the temperature, which is confirmed experimentally (see Fig. 25). The frequencies of all $\Gamma_1 - \Gamma_4$ excitations (see Fig. 25) remain finite for finite values of q , and also at the edge of the band ($q = 0$), i.e., they do not soften completely as $T \rightarrow T_{\text{cr}}$. The same occurs for TbSb . In contrast to this, the transverse excitations within the triplet Γ_4 soften as $T \rightarrow T_{\text{cr}}$ and disappear (see Fig. 25) as a result of the degeneracy of the triplet as $T \rightarrow T_{\text{cr}}$. These triplet excitations lead to a divergence of the transverse static susceptibility. Since the order parameter in these induced magnetic systems is $\langle J_z \rangle$, the longitudinal static susceptibility must diverge near the phase transition. However, soft inelastic longitudinal excitations have not been found.

Smith and Buyers,⁶⁵ using molecular-field-random-phase calculations for a singlet-triplet system with allowance for the complete level scheme, argue that the dynamics of the phase transition for systems with singlet ground state and with degenerate excited state of corresponding symmetry differs fundamentally from that in the simple singlet-singlet model. They predict that the phase transition in the system Pr_3Tl (singlet-triplet) must be characterized by a central peak with divergent intensity at $T \rightarrow T_{\text{cr}}$ due to $\omega = 0$ critical scattering. This is confirmed by neutron inelastic scattering experiments on TbSb , PrTl , and PrAl_2 (see Figs. 18, 19, and 21). A divergent central peak is also observed for the Jahn-Teller phase transition,⁹⁰ which is ascribed to a similar electron effect. To explain the effects observed in the PrAl_2 dispersion curves (repulsion of the phonon and magnetic branches), it is necessary to take into account the influence of the acoustic phonons on the magnetically interacting system (see Sec. 3.3.2),^{70,75,91} and also the anisotropy in the mag-

netic exchange.⁷⁶

To gain a better understanding of the induced magnetic phase transition, it is desirable to make inelastic neutron-scattering investigations into the temperature dependence of the magnetic excitations and the central peak in other substances (if possible, single crystals) such as PrMg_2 , PrGa_2 , PrZn , Pr_3In , PrNi_2 . Further, it is necessary to develop a self-consistent molecular-field theory for the theoretical description of phase transitions with allowance for fluctuations (for example, a self-consistent random-phase theory).

3.2. Systems with structural instability

It will be shown here for the example of several substances that crystal-field effects play an important part in the elastic properties of metallic rare-earth compounds. To analyze the temperature dependence of the macroscopic properties (specific heat, elastic constants, and so forth), it is necessary to know the splitting of the electron multiplets in the crystal field, obtained, for example, by means of inelastic neutron scattering.

The basic mechanism for the cooperative Jahn-Teller effect is the change produced by the small displacements of the ions of the ligands in the crystal field acting on the Jahn-Teller active ion. Expanding the Hamiltonian of the crystal field in the displacements of the ligands, we obtain ultimately an effective coupling of quadrupole type between the rare-earth ions, the coupling being transmitted through the system of phonons.^{70,75} In metallic systems, these displacements of the ligands (phonons) interact additionally with the conduction electrons, which, in their turn, interact through elastic and inelastic Coulomb scattering with the rare-earth ions, so that the quadrupole interaction between the ions of the rare-earth elements in the metallic systems is enhanced.

The important features of the quadrupole interaction are as follows⁶⁷:

- the quadrupole-quadrupole QQ interaction is realized through the conduction electrons and the phonons;
- an external stress field (homogeneous or inhomogeneous) makes it possible to study these interactions;
- ions with nonmagnetic doublet ground state (for example, Γ_3 for cubic point symmetry of the rare-earth ions) always exhibit a cooperative Jahn-Teller phase transition at sufficiently low temperature;
- in the case of a singlet ground state, as induced Jahn-Teller phase transition occurs if the QQ interaction is sufficiently strong.

The ordered phase (quadrupole ordering) in a system with structural phase transition can be treated theoretically in the same way as in the case of an ordered magnetic state.⁶⁷

3.2.1. Induced structural transition. In contrast to nonconducting compounds, there is as yet only one representative in the metallic system which exhibits an induced collective Jahn-Teller phase transition.¹⁰⁴ The

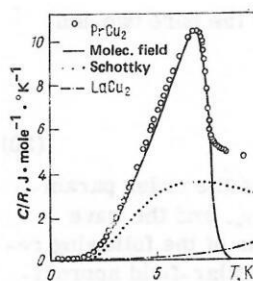


FIG. 26. Temperature dependence of the specific heat of PrCu_5 .¹⁰⁷

intermetallic compound PrCu_2 , for which magnetic electron ordering has not been observed down to 1°K,¹⁰⁵ has orthorhombic structure of CeCu_2 type (Imma) with four equivalent Pr ions in the unit cell. The ground-state $^3\text{H}_4$ multiplet is completely split, and there exist only singlet states. Hitherto, inelastic neutron-scattering measurements have not been made with this substance. Quite generally, such systems with crystal field and low symmetry have very complicated spectra because of the large number of possible transitions.

In connection with the obtaining of low temperatures by adiabatic demagnetization, the compound PrCu_2 is of interest because of the possibility of finding nuclear magnetic ordering at relatively high temperatures (several millikelvin) as a result of hyperfine coupling of the nuclear moments.¹⁰⁶ It follows from the temperature dependence of the specific heat and the magnetic susceptibility that nuclear magnetic ordering occurs at 54 m°K,¹⁰⁵ and, in addition, the specific heat exhibits a well-defined peak at $T = 6^\circ\text{K}$. The new measurements of Ref. 107 confirmed the anomaly at 7.5°K (Fig. 26). Judging from the magnitude and form (sharp peak) of the anomaly, one would expect a Schottky anomaly and Jahn-Teller transition to be responsible for it. This is confirmed both by measurements of the magnetic susceptibility and measurements of the temperature dependence of the linear expansion coefficients along the three principal axes (Fig. 27).¹⁰⁴ From this there follows a scheme of the levels for the three lowest singlets at energies 0, 0.52, and 1.55 meV, a quadrupole coupling being manifested between only the two lowest levels.

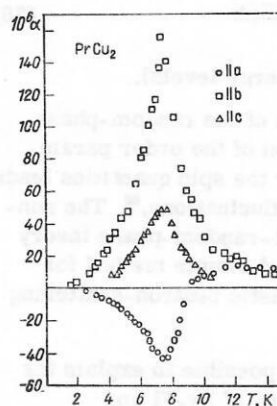


FIG. 27. Temperature dependence of the coefficient of linear expansion α in PrCu_2 along the axes a, b, c.¹⁰⁴

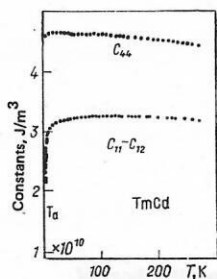


FIG. 28. Temperature dependence of the elastic moduli c_{44} and $c_{11} - c_{12}$ in TmCd (the frequency was 10 MHz).¹⁰⁸

3.2.2. Cooperative Jahn-Teller phase transition in the case of a degenerate ground state. In the TmCd system, a structural phase transition at $T = 3.16^\circ\text{K}$ has been found and attributed to the Jahn-Teller effect.¹⁰⁸ It was concluded from the behavior of the elastic constants (Fig. 28) that there is a cooperative Jahn-Teller phase transition without additional occurrence of magnetic ordering. This last conclusion followed from measurements of the magnetic susceptibility up to $40\text{ m}^\circ\text{K}$ (typical Van Vleck behavior).

The phase transition is from cubic (CsCl type) to tetragonal structure. It follows from measurements of the specific heat (Fig. 29) that the phase transition is of the first kind. The temperature dependence of the macroscopic properties for $T < 100^\circ\text{K}$ is strongly influenced by the crystal field. It follows from the specific heat and the resistivity for the ground-state 3H_6 multiplet of the ion Tm^{3+} that the ground state is a non-magnetic Γ_3 doublet, and the first excited level must lie at 20°K . Unfortunately, the compound TmCd is completely unsuitable for inelastic neutron-scattering experiments because of the large cross section of capture of thermal neutrons by cadmium. Therefore, a direct determination of the splitting by the crystal field was not made, which is a disadvantage for interpreting the measured macroscopic effects.

The temperature dependence of the elastic moduli $c_{11} - c_{12}$ exhibits strong softening. The absorption near the phase transition is so strong that one cannot obtain values in the immediate proximity of the transition (see Fig. 28). The c_{44} branch also reveals a small dip near T_a with a subsequent rise. For a quadrupole coupling of the elastic branches and QQ interaction of the Jahn-Teller ions, the experiments can be excellently interpreted in the molecular-field approximation with allowance for the entire level scheme. From the fact that

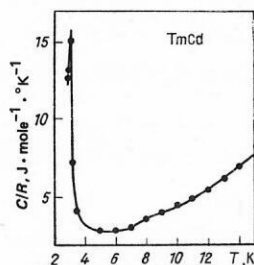


FIG. 29. Temperature dependence of the specific heat C/R in TmCd.¹⁰⁸

the phase transition is of the first kind (deduced from the specific heat) it is concluded that at least part of the QQ interaction is of short range.

In addition, it was noted for the first time that application of a magnetic field in the presence of a structural phase transition of the first kind shifts the transition point to higher temperatures.¹⁰⁸

3.3 Systems with magnetic and structural phase transitions

Depending on the ratio $K(0)/I(0)$ of the exchange coupling constants for the quadrupole-quadrupole and magnetic dipole-dipole interactions, a system may exhibit both magnetic and structural phase transitions. If the constant $K(0)$ is sufficiently large, then (with decreasing temperature) there occurs first a cooperative Jahn-Teller phase transition, which is followed at a lower temperature by a magnetic phase transition. At a structural phase transition of the second kind, the corresponding elastic branches soften. If the magnetic phase transition occurs first [$I(0)$ is sufficiently large], then in the case of weak magnetoelastic coupling (the coupling between the magnetic and phonon systems) comparatively small changes in the elasticity constants occur near the phase transition. If, conversely, the magnetoelastic interaction is large, then the two phase transitions (magnetic and structural) can occur simultaneously at the same temperature. Such a coupled phase transition is also accompanied by a softening of the elementary excitations of corresponding symmetry.

In the ordered magnetic phase, the ground state of the ion will always have, in addition to a magnetic dipole moment, a quadrupole moment, and therefore the symmetry of the magnetic state will be lower. The opposite assertion is not necessarily true because in the case of a quadrupole phase transition the ground state with quadrupole moment need not necessarily have a magnetic moment (for example, Γ_3 in the cubic case).

3.3.1. Structural and magnetic phase transitions at the same temperature. In intermetallic compounds of rare-earth elements with NaCl and CsCl structure a magnetic phase transition is frequently accompanied at the same temperature $T_a = T_N, T_C$ by a structural instability. This occurs, for example, in TbX ($X = \text{P, As, Sb}$).^{71,109} Theoretically, such a phase transition is of the first kind.¹¹⁰ In other pnictides of the rare-earth elements (Pr, Tm), the exchange and quadrupole interactions are insufficiently strong to cause magnetic and structural phase transitions. Figure 30 shows the magnetic contribution to the specific heat in TbP. There is a strong peak at $T = 7.08^\circ\text{K}$ and a broad Schottky anomaly at 10°K . Analyzing these data, one can obtain crystal-field parameters in good agreement with the results of inelastic neutron-scattering experiments.²¹ The sharp peak in the specific heat in Fig. 30 indicates a phase transition of the first kind. Such a conclusion is confirmed by x-ray structural investigations⁴¹¹ and measurements of the elastic constants.⁷¹ The absence of a second peak in the curve of the specific heat together with the appearance of an elastic anomaly at the same temperature (Fig. 31) confirms that in TbP the structural and magnetic phase

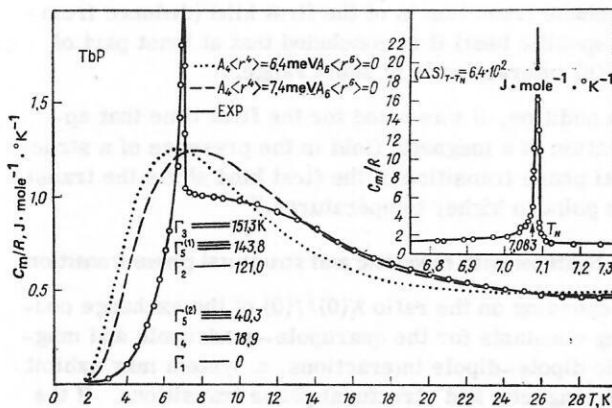


FIG. 30. Temperature dependence of the specific heat in TbP. The broken curves correspond to a calculation of the Schottky anomaly with the crystal-field parameters indicated in the figure. The level scheme corresponds to the curve with long dashes. In the top right, the difference between the experimental and calculated curves.²¹

transitions coincide. The same has been observed in DySb,¹¹² HoSb,¹¹³ and also in TbZn, DyZn, TbCu.¹¹⁴ Figure 31 shows the results of measurements of the velocity of sound for the branch c_{44} in TbP.

As a result of trigonal distortions,¹⁰⁹ a softening by ~8% in the velocity of sound was also observed. At $T_N = 7^\circ\text{K}$, the softening ceases because of the magnetic phase transition.

3.3.2. Magnetic and structural phase transitions at different temperatures. The metallic compounds of the rare-earth elements with zinc have a strong magneto-elastic coupling. This has the consequence that the magnetic phase transition occurs at the same temperature as the structural phase transition (see 3.3.1). The only exception is TmZn,¹¹⁴ which is ordered structurally (Jahn-Teller phase transition) and magnetically at different temperatures ($T_C = 8.12^\circ\text{K}$, $T_A = 8.55^\circ\text{K}$). The results of measurements of the specific heat are shown in Fig. 32. Confirmation is provided by investigations of the temperature dependence of the elastic moduli $c_{11}-c_{12}$ ¹¹⁵ and of the magnetization and resistivity.¹¹⁴ The results of experiments on inelastic neutron scattering show that the ground state of the Tm^{3+} ion is a magnetic triplet Γ_5 . The scheme of the crystal-field levels is as follows: $\Gamma_5^1(0)$, $\Gamma_3(3.3 \text{ meV})$, $\Gamma_4(14.6 \text{ meV})$, $\Gamma_1(16.3 \text{ meV})$, $\Gamma_5^2(17.3 \text{ meV})$, $\Gamma_2(21.7 \text{ meV})$. This corresponds to the following set of Lea-Leask-Wolf parameters: $X = (-0.31 \pm 0.02) \text{ meV}$ and $W = (0.103 \pm 0.01) \text{ meV}$. Figure 33 shows the temperature dependence of

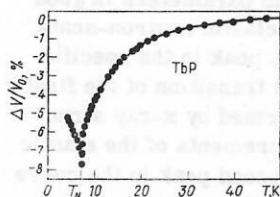


FIG. 31. Temperature dependence of the relative velocity of sound for the branch c_{34} . The points are the experimental data from Ref. 109.

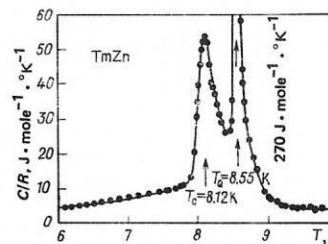


FIG. 32. Temperature dependence of the specific heat of TmZn.¹¹⁴

the intensities of some of the crystal-field transitions, from which the above level scheme was deduced.¹¹⁴

To describe theoretically the rare-earth systems considered in Sec. 3.3 with magnetic and structural phase transitions, it is necessary to include the appropriate interactions in the Hamiltonian. The general scheme of the molecular-field-random-phase description (see Sec. 3.1.3) is not changed. The Hamiltonian consists of the parts

$$H = H_{cf} + H_{exc} + H_{int}^{JT} + H_{me} + H_{ph}. \quad (37)$$

The first three terms of the Hamiltonian have already been considered. The part H_{ph} describes the vibrations of the lattice around the equilibrium position in the harmonic approximation.

The magnetoelastic part H_{me} couples the phonon system to the magnetically interacting system. It is considered in detail in Refs. 70, 75, and 91.

In the framework of the non-self-consistent theory in the molecular-field-random-phase approximation the coupled spectrum of elementary excitations is calculated from the poles of the phonon or the spin Green's function.

Unfortunately, for metallic compounds of the rare-earth metals with structural instability and also for systems with coupled phase transition, no inelastic neutron-scattering investigations have yet been made of the spectrum of elementary excitations (phonon-

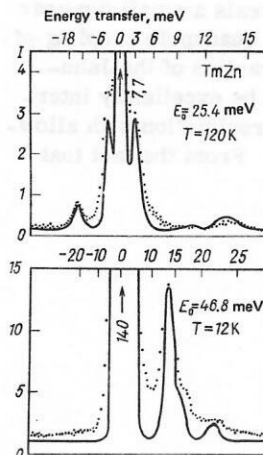


FIG. 33. Time-of-flight spectrum for inelastic neutron scattering. The curves are the calculation of Ref. 114 and the points are the experimental results.

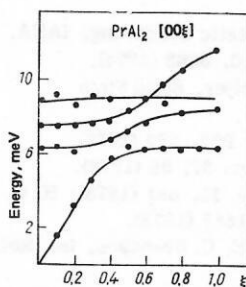


FIG. 34. Dispersion curves of magnetoelastic excitations in PrAl_2 in the $[0, 0, \xi]$ direction. The points are from the experiment of Ref. 91.

magnetic excitation). However, in the PrAl_2 system, in which there are no structural phase transitions and the magnetoelastic interaction plays a large part, an influence of acoustic phonons on the magnetic excitations has been observed (see Fig. 34; direction $[00\xi]$, with $\xi \approx 0.5$). The simple model (34) makes it possible to interpret such spectra of mixed elementary excitations.¹¹⁶ The excitation energies must be the same in both nuclear and magnetic scattering of the neutrons. The calculated dispersion dependence of the magnetoelastic excitations in the ferromagnetic phase of PrAl_2 at $T = 4.4^\circ\text{K}$ agrees well with the experimental dependence (see Fig. 33).⁹¹ It has also not yet been possible to find quadrupole excitations in metallic Jahn-Teller systems by means of inelastic neutron scattering. Such a possibility is offered by experiments with inelastic scattering of polarized neutrons at large momentum transfers.¹¹⁶

It should be noted that significant progress has recently been achieved in the investigation of crystal-field effects of rare-earth intermetallics by means of inelastic neutron scattering. However, the splitting of the $5f$ multiplets in the metallic compounds of the actinides has hardly been studied by means of inelastic neutron scattering. This is because the $5f$ electrons of the actinides are not so strongly localized as the $4f$ electrons of the rare-earth intermetallics and a state of intermediate valence may also occur.

There have also been some inelastic neutron-scattering studies of the spin and lattice dynamics with a view to elucidating the nature of the magnetic and structural phase transitions, but no measurements of the temperature dependence of the phonon branches near a structural phase transition have yet been made.

Considering the results presented in the paper, we should consider the most important directions in future experimental and theoretical studies:

a) determination of the complete splitting of the ground-state multiplet in the crystal field of the metallic compounds of the actinides and study of the mixed valence states by quasielastic and inelastic neutron scattering;

b) study of the dynamics of magnetic and structural phase transitions, determination of the temperature dependence of the phonon and magnetic branches and the hybridization of the magnetic elementary excitations with the phonons.

CONCLUSIONS

The study of the splitting of electron multiplets by means of inelastic neutron scattering began ten years ago. Since 1970, such experiments have been made with the pulsed reactor IBR-30 at the Laboratory of Neutron Physics at the JINR, Dubna. This work was initiated by F. L. Shapiro. Initially, investigations were made on the insulators PrF_3 , PrFeO_3 , and PrGaO_3 . From the middle of the seventies, a start was made on the investigation of the metallic compounds of rare-earth metals. The alloys Pr_3Al , PrAl_2 , PrAl_3 , PrMg , PrMg_3 , PrNi_5 , PrCu_5 , and PrNi_2 were investigated.

Experiments using the time-of-flight technique with the pulsed reactor IBR-30 have certain advantages over neutron-scattering experiments with stationary reactors, particularly with regard to the study of the high-energy crystal-field levels. With the commissioning of the IBR-2, the possibilities of studying the crystal field are extended. The region of energy transfers 200–300 meV becomes accessible with good resolution, which is particularly important in the investigation of the metallic systems of the actinides and the elementary excitations of the $3d$ transition metals and alloys.

¹A. E. Siegman, *Microwave Solid State Masers*, McGraw-Hill, New York (1964).

²S. V. Vonsovskii, *Magnetizm (Magnetism)* [in Russian], Nauka, Moscow (1971).

³W. M. Yen, W. C. Scott, and A. L. Schawlow, *Phys. Rev. A* **136**, 271 (1964).

⁴A. Hadni and P. Strimer, *Phys. Rev. B* **5**, 4609 (1972).

⁵E. Y. Wong, O. M. Stafsudd, and D. R. Johnston, *J. Chem. Phys.* **39**, 786 (1963).

⁶K. N. R. Taylor and M. I. Darby, *Physics of Rare Earth Solids*, Chapman, London (1973).

⁷A. J. Freeman and R. E. Watson, *Phys. Rev.* **127**, 2058 (1962).

⁸H. H. Andersen *et al.*, *Phys. Rev. Lett.* **32**, 1321 (1974).

⁹W. E. Wallace, *Rare Earth Intermetallics*, Academic Press, New York (1973), Chap. 3.

¹⁰R. K. Lea, M. J. M. Leask, and W. P. Wolf, *J. Phys. Chem. Solids* **23**, 1381 (1962).

¹¹E. Segal and W. E. Wallace, *J. Solid State Chem.* **2**, 347 (1970).

¹²M. T. Hutchings, in: *Solid State Physics*, Vol. 16, Academic Press, New York (1964), p. 227.

¹³W. B. Lewis, in: *Magnetic Resonance and Related Phenomena*, Proc. XVI Congress AMPERE, Bucharest (1971), p. 717.

¹⁴W. Marshall and S. W. Lovesey, *Theory of Thermal Neutron Scattering*, Clarendon Press, Oxford (1971).

¹⁵P. G. De Gennes, in: *Magnetism*, Vol. 3, Academic Press, New York (1963), p. 115.

¹⁶E. Blacar and S. W. Lovesey, *Phys. Lett. A* **31**, 67 (1970).

¹⁷*Crystal Field Effects in Metals and Alloys*, Plenum Press, New York (1977).

¹⁸R. J. Birgeneau *et al.*, *Appl. Phys.* **41**, 900 (1970).

¹⁹K. C. Turberfield *et al.*, *J. Appl. Phys.* **42**, 1746 (1971).

²⁰R. J. Birgeneau *et al.*, *Phys. Rev. B* **4**, 719 (1971).

²¹R. J. Birgeneau *et al.*, *Phys. Rev. B* **8**, 5345 (1973).

²²A. Furrer *et al.*, in: *Neutron Inelastic Scattering*, Proc. Symposium, Grenoble, 1972, IAEA, Vienna (1972), p. 563.

²³A. Furrer and E. Warming, *J. Phys. C* **7**, 3365 (1974).

²⁴A. Furrer and U. Tellenbach, *Phys. Status Solidi B* **71**, K31 (1975).

- ²⁵A. Furrer and W. Halg, *J. Phys. C* **9**, 3499 (1976).
- ²⁶A. Furrer, J. Kjems, and O. Vogt, *J. Phys. C* **5**, 2246 (1972).
- ²⁷M. M. Ellis and D. J. Newman, *J. Chem. Phys.* **49**, 4937 (1968).
- ²⁸E. Bucher and J. P. Maita, *Solid State Commun.* **13**, 215 (1973).
- ²⁹W. Gordy and W. J. O. Thomas, *J. Chem. Phys.* **24**, 439 (1956).
- ³⁰J. Rossat-Mignod *et al.*, in: 11th Rare Earth Research Conf., Vol. 1, Traverse City (1974), p. 317.
- ³¹P. Morin *et al.*, *Phys. Rev. B* **9**, 4932 (1974).
- ³²P. Morin *et al.*, *J. Phys.* **37**, 611 (1976).
- ³³D. Schmitt, P. Morin, and J. Pierre, *Phys. Rev. B* **15**, 1968 (1977).
- ³⁴P. Morin and J. Pierre, *Phys. Status Solidi A* **30**, 549 (1975).
- ³⁵P. Morin *et al.*, *Solid State Commun.* **25**, 265 (1978).
- ³⁶P. Morin, J. Rouchy, E. du Tremolet de Lacheisserie, *Phys. Rev. B* **16**, 3182 (1977).
- ³⁷D. Schmitt, *J. Phys. F* **7**, 1521 (1977).
- ³⁸A. Furrer, *J. Phys. C* **8**, 824 (1975).
- ³⁹U. Tellebach, A. Furrer, and A. H. Millhouse, *J. Phys. C* **8**, 3833 (1975).
- ⁴⁰T. O. Brun *et al.*, *Phys. Rev. B* **9**, 248 (1974).
- ⁴¹K. N. R. Taylor, *Adv. Phys.* **20**, 551 (1971).
- ⁴²A. Furrer *et al.*, *Int. Magnetism* **4**, 63 (1973).
- ⁴³H. Heer *et al.*, *J. Phys. C* **7**, 1207 (1974).
- ⁴⁴H. -G. Purwins *et al.*, *Helv. Phys. Acta* **45**, 20 (1972).
- ⁴⁵H. Happel *et al.*, in: Ref. 17.
- ⁴⁶K. Hennig *et al.*, *Solid State Commun.* **21**, 297 (1977); T. Frauenheim, W. Matz, and G. Feller, *Solid State Commun.* **29**, 805 (1979).
- ⁴⁷W. Bührer *et al.*, *Solid State Commun.* **13**, 881 (1973).
- ⁴⁸J. G. Houmann *et al.*, *J. Phys. C* **7**, 2691 (1974).
- ⁴⁹H. -G. Purwins *et al.*, in: AIP Conf. Proc. **23**, 259 (1976).
- ⁵⁰H. -G. Purwins *et al.*, *J. Phys. C* **7**, 3573 (1974).
- ⁵¹H. -G. Purwins *et al.*, *J. Phys. C* **9**, 1025 (1976).
- ⁵²W. Matz, Dissertation, TU Dresden (1978).
- ⁵³P. Lethuillier and J. Chaussy, *J. Phys. (Paris)* **37**, 123 (1966).
- ⁵⁴A. Furrer and H. -G. Purwins, *J. Phys. C* **9**, 1491 (1976).
- ⁵⁵W. Gross *et al.*, in: Ref. 17.
- ⁵⁶A. Furrer, A. Murasik, and Z. Kletowski, in: Ref. 17.
- ⁵⁷P. Lethuillier, in: Ref. 17.
- ⁵⁸P. A. Alekseev *et al.*, *Fiz. Tverd. Tela (Leningrad)* **18**, 676, 2509 (1976).
- ⁵⁹J. V. Mahoney and A. Furrer, *Neutronenstreuung*, Progress Report AF-SSP-80, Institut für Reaktortechnik, Würenlingen, Zurich (1974), p. 37.
- ⁶⁰A. Andreeff *et al.*, *Phys. Status Solidi B* **87**, 535 (1978).
- ⁶¹A. P. Murani, K. Knorr, and K. H. J. Buschow, in: Ref. 17.
- ⁶²P. A. Alekseev *et al.*, *Phys. Status Solidi B* **97**, 87 (1980).
- ⁶³M. A. Ruderman and C. Kittel, *Phys. Rev.* **96**, 99 (1954).
- ⁶⁴Th. Frauenheim and G. Ropke, *Phys. Status Solidi B* **88**, 457 (1978).
- ⁶⁵W. J. L. Buyers, AIP Conf. Proc. **24**, 27 (1974); W. J. L. Buyers, T. M. Holden, and A. Perreault, *Phys. Rev. B* **11**, 266 (1975).
- ⁶⁶G. A. Gehring and K. A. Gehring, *Rep. Prog. Phys.* **38**, 1 (1975).
- ⁶⁷P. Fulde, in: *Handbook on the Physics and Chemistry of Rare Earths*, North-Holland, Amsterdam (1978), p. 295.
- ⁶⁸R. J. Elliot *et al.*, *Proc. R. Soc. London, Ser. A* **338**, 217 (1972); B. Luthi, M. E. Mullen, and E. Bucher, *Phys. Rev. Lett.* **31**, 95 (1973).
- ⁶⁹P. Fulde and I. Peschel, *Adv. Phys.* **21**, 1 (1972); P. Fulde, *Z. Phys. B* **20**, 89 (1975).
- ⁷⁰V. Dohm and P. Fulde, *Z. Phys. B* **21**, 369 (1975).
- ⁷¹E. Bucher *et al.*, *Z. Phys. B* **25**, 41 (1976).
- ⁷²L. L. Hirst, *Z. Phys.* **224**, 230 (1971).
- ⁷³T. H. Holden *et al.*, in: *Neutron Inelastic Scattering*, IAEA, Vienna (1977), p. 553; *Phys. Rev. B* **10**, 3863 (1974).
- ⁷⁴Th. Frauenheim, W. Matz, and G. Feller, *Solid State Commun.* **29**, 805 (1979).
- ⁷⁵P. Thalmeier and P. Fulde, *Z. Phys. B* **22**, 359 (1975).
- ⁷⁶P. -A. Lindgard, *Inst. Phys. Conf. Ser.* **37**, 96 (1978).
- ⁷⁷W. Bührer *et al.*, *Solid State Commun.* **13**, 881 (1973); H. G. Purwins *et al.*, *Phys. Rev. Lett.* **31**, 1585 (1973).
- ⁷⁸T. W. Holden, W. J. L. Buyers, and E. C. Svensson, in: Ref. 17.
- ⁷⁹R. J. Birgeneau, J. Als-Nielsen, and E. Bucher, *Phys. Rev. Lett.* **27**, 1530 (1971).
- ⁸⁰J. Als-Nielsen *et al.*, *J. Phys. C* **10**, 2673 (1977).
- ⁸¹K. Niiara, *Phys. Rev.* **117**, 129 (1960); B. R. Cooper *et al.*, *Phys. Rev.* **127**, 57 (1962).
- ⁸²T. Holstein and H. Primakoff, *Phys. Rev.* **58**, 1098 (1940).
- ⁸³T. M. Holden and M. J. L. Buyers, *Phys. Rev. B* **9**, 3797 (1974).
- ⁸⁴R. J. Birgeneau, AIP Conf. Proc. **10**, 1664 (1973); R. J. Birgeneau, L. Als-Nielsen, and E. Bucher, *Phys. Rev. B* **6**, 2724 (1972).
- ⁸⁵W. J. L. Buyers *et al.*, *J. Phys. C* **4**, 2139 (1971).
- ⁸⁶I. Peschel, M. Klenin, and P. Fulde, *J. Phys. C* **5**, L194 (1972).
- ⁸⁷S. V. Tyablikov, *Metody kvantovoi teorii magnetizma*, Nauka, Moscow (1975); English translation: *Method of Quantum Theory of Magnetism*, Plenum, New York (1967).
- ⁸⁸Th. Frauenheim and J. Schreiber, Preprint R17-11978 [in Russian], JINR, Dubna (1978).
- ⁸⁹S. R. Smith, *J. Phys. C* **5**, 157 (1972).
- ⁹⁰M. T. Hutchings *et al.*, *J. Phys. C* **8**, 393 (1975).
- ⁹¹V. L. Aksenov *et al.*, Preprint R17-12962 [in Russian], JINR, Dubna (1979).
- ⁹²A. Furrer and H. G. Purwins, *Phys. Rev. B* **16**, 2131 (1977).
- ⁹³B. Hennion *et al.*, in: Ref. 17.
- ⁹⁴A. Furrer, P. H. Levy, and E. Kaldis, in: Ref. 17.
- ⁹⁵J. J. Rhyne, S. J. Pickart, and H. A. Alperin, AIP Conf. Proc. **18**, 5631 (1973).
- ⁹⁶J. J. Rhyne *et al.*, *Physica (Utrecht)* **B86**, 149 (1977); *Physica (Utrecht)* **C86-88**, 149 (1977).
- ⁹⁷R. H. Nicklow *et al.*, *Phys. Rev. Lett.* **36**, 532 (1976).
- ⁹⁸J. J. Rhyne and N. C. Koon, *J. Appl. Phys.* **49**, 2133 (1978).
- ⁹⁹J. G. Houmann and H. B. Moller, in: *Proc. of the Conf. on Neutron Scattering*, Gatlinburg (1976), p. 743.
- ¹⁰⁰J. G. Houmann, M. J. L. Buyers, and A. R. Mackintosh, *Riso Report N 334* (1975), p. 18.
- ¹⁰¹A. Furrer *et al.*, *Phys. Rev. B* **14**, 179 (1976).
- ¹⁰²J. Pierre *et al.*, *J. Phys. (Paris)* **39**, 793 (1978).
- ¹⁰³C. Yetteir *et al.*, *Phys. Rev. Lett.* **39**, 1028 (1977).
- ¹⁰⁴H. R. Ott *et al.*, in: Ref. 17, p. 84.
- ¹⁰⁵K. Andres, *Cryogenics* **18**, 473 (1978).
- ¹⁰⁶K. Andres *et al.*, *Phys. Rev. Lett.* **28**, 1652 (1972).
- ¹⁰⁷M. Wun and M. E. Phillips, *Phys. Lett. A* **50**, 195 (1974).
- ¹⁰⁸B. Luthi *et al.*, *Phys. Rev. B* **8**, 2639 (1973).
- ¹⁰⁹F. Levy, *Phys. Kondens. Mater.* **10**, 85 (1969).
- ¹¹⁰P. Bak, S. Krinsky, and D. Mukamel, *Phys. Rev. Lett.* **36**, 52 (1976).
- ¹¹¹E. Bucher *et al.*, *Phys. Rev. Lett.* **28**, 746 (1972).
- ¹¹²M. E. Mullen *et al.*, *Phys. Rev. B* **10**, 136 (1974).
- ¹¹³P. Morin, Thesis, University of Grenoble, CNRS, A. O. 9323 (1975).
- ¹¹⁴P. Morin, J. Rouchy, and D. Schmitt, *Phys. Rev. B* **17**, 3684 (1978).
- ¹¹⁵P. Morin, A. Waintal, and B. Luthi, *Phys. Rev. B* **14**, 2972 (1976).
- ¹¹⁶P. M. Levy and G. T. Teamell, *J. Phys. C* **10**, 1203 (1977).

Translated by Julian B. Barbour